Supplementary Materials for

Endemic persistence of a highly contagious pathogen: Foot-and-mouth disease in its wildlife host

Anna Jolles *et al.*

Corresponding author: Anna Jolles, aejolles@gmail.com

The PDF file includes:

Materials and Methods
Supplementary Text S1 to S6
Figs. S1 to S13
Tables S1 to S7
References

Other Supplementary Material for this manuscript includes the following:

MDAR Reproducibility Checklist

Materials and Methods

Cohort study

Our cohort study operated in a 900ha enclosure in the central Satara section of Kruger National Park, South Africa, surrounded by a double fence designed to prevent disease transmission between animals within and outside the enclosure. The study has been previously described [54,55]. Briefly, the study herd included 49-70 animals of mixed age and sex, varying due to natural births and deaths during the study period. The herd was originally established in 1998, when animals were captured in the northern KNP and released into the enclosure for a TB-free breeding project. That project ended in 2007, but a founder herd of TB-free buffalo remained in the Satara enclosure. The herd remained largely isolated, but occasional break-ins by buffalo being pushed to the fence by lions did occur (two known events in 2013 and 2016); and ten females and their calves were captured in the Satara section and added to the herd in 2016. The study herd was minimally managed, grazing and breeding naturally, and finding water at natural pans and man-made water troughs. During extreme dry seasons, supplemental grass and alfalfa hay were supplied to the buffalo. The herd enclosure excluded megaherbivores (elephant, rhino, hippo) and large predators (lion, leopard, hyena), but otherwise included a typical assemblage of mammalian savanna species. The entire buffalo herd was captured every 2-3 months between February 2014 and August 2017 (17 capture periods in total; 108 unique individuals sampled longitudinally for 1104 observations). Capture and sedation procedures have been previously described [54,55]. At each capture, blood was collected from each individual to quantify FMDV-specific antibodies (see FMDV diagnostic testing, below). Tissue samples were taken from each individual once, for DNA extraction to assess relatedness between mom-calf pairs. After each capture, and at the end of the study, the herd was released back into their enclosure. Our study included three calf cohorts [N(2013-14)=16, N(2014-15)=14, N(2015-16)=4] sampled at the same time as the rest of the herd. The birth date of each calf was estimated by backdating from their age at first capture, and mother-calf pairs were identified by genotyping[54]. No calves were born / surviving to first capture in 2016-17. The high rate of abortions/ reabsorption that year probably accounts for the recruitment failure; there was no evidence of brucellosis infection.

Experimental study

We used established protocols[16] to infect 12 buffalo with FMDV via intralingual infection - four animals per serotype (SAT1, SAT2, or SAT3) using the same viruses isolated from buffalo in Kruger National Park Park, KNP/196/91/1 PK1 RS5, KNP/19/89/2 PK1 RS4, and KNP/1/08/3 PK1 RS4 (Genbank accession numbers KR108948, KR108949 and KR108950). Animals were randomly assigned to treatment groups, and buffalo infected with each serotype were kept in separate pens at the State Veterinary animal facility in Skukuza, within the park, and infection status was confirmed using viral RNA detection. To assess transmission of FMDVs during acute infection, we allowed 12 naive buffalo (adding four to each pen of infected buffalo) to mix with the recently infected animals after two days (Fig. S4a). The 12 recipient animals were sedated on days 2, 4, 6, 8, 11, 14 and 30 days post FMDV exposure to allow for collection of blood samples for quantification of FMDV viremia and antibody responses. “Probang” samples (oropharyngeal scrapings containing fluid and epithelial cells) and palatine tonsil swab samples were collected to detect virus.

To quantify transmission from carrier buffalo to naive hosts, we used the four contact-infected buffalo for each serotype as carriers, split the carriers into two groups, and housed each group of six (2xSAT1, 2xSAT2, 2xSAT3) carriers with six naive animals (Fig. S4b. Carrier status of the contact-infected animals was confirmed by testing for viral RNA in probang and tonsilar swab samples (see FMDV diagnostic testing). Since prior exposure to one serotype does not preclude infection with a second, heterologous, FMDV serotype [8,16,24,56], each group thus contained ten animals susceptible to each serotype. Buffalo were sampled to assess FMDV transmission (see FMDV diagnostic testing, below) from the carrier animals two weeks after contact between carriers and naïve buffalo, and subsequently monthly, for a total of 6.5 months. Test results are summarized in Fig. S5.

Throughout the experimental study, animal welfare was monitored daily by State Veterinary Services employees (assessing feed intake and a visual assessment of health status such as alertness and responsiveness), and at each immobilization event by veterinarians (assessing weight gain, performing a full physical examination, monitoring of infectious diseases). As per agreement under Section 20 of the Animal Diseases Act (Act 35 of 1984) with the South African Department of Agriculture, the experimental animals were humanely euthanized at the end of the experiment, to ensure that FMD viruses used in experimental infections are not introduced into any natural population.

FMDV diagnostic testing

Classification of animals: (i) Maternally protected: High initial antibody titres in calves observed in the cohort study were interpreted as maternally-derived antibodies, if the mother also was seropositive for that serotype of FMDV. The following were distinguished during the experimental study: (ii) Susceptible: Buffalo were considered susceptible if no viral RNA was detected in blood, probang, or tonsillar swab samples, and FMDV-specific antibodies were not detected in their serum (iii): Infectious: Buffalo were assumed to be infectious if viral RNA was detected in their blood(47). (iv) Carriers: Animals were considered carriers, if viral RNA could be isolated from tonsil swabs or probang samples 28 days post infection[57]. (v) Recovered: Buffalo were considered recovered if they had a protective antibody titer against a given viral serotype, but did not carry the virus.

Sampling: For both cohort and experimental studies, blood, tonsillar swabs and probang samples were collected at the time of capture. Whole-blood samples were collected from the jugular vein into 10 ml, plain evacuated tubes with no additives (Vacutainer® tubes). The blood was allowed to clot at ambient temperature and then centrifuged at 3000 rpm for 10 min. Serum was decanted into sterile cryovials immediately after centrifugation and stored at -20°C until testing. OPF sampling was performed according to Kitching and Donaldson[58], diluted in 3 ml probang buffer and snap frozen. The tonsilar crypts were swabbed individually using nylon brushes (Cytotak Transwab)[59]. Laryngoscopes used to depress the tongue, gags and all other equipment in contact with the animal were disinfected in citric acid and rinsed in PBS after each animal was sampled. Nylon brushes were transferred to 0.5ml probang buffer and snap frozen in liquid nitrogen. At processing, cryotubes were vortexed and centrifuged as described previously[16]. Duplicate sets of samples were transported to the Transboundary Animal Disease (TAD) Laboratory of the ARC-Onderstepoort Veterinary Institute (ARC-OVI) in Pretoria, and to the Pirbright Institute (TPI), UK, for testing.

Viral RNA detection by real-time quantitative RT-PCR: RNA detection was performed at ARCOVI (South Africa) and the Pirbright Institute (TPI, UK), and results cross-validated for both labs. (i) ARC-OVI: The viral RNA in probang samples, tonsil swabs and whole blood was detected using a one-step real-time RT-PCR assay targeting the 3D region[60], tested in duplicate. Total RNA was extracted using QIAamp Viral RNA Mini Kit (Qiagen), according to the manufacturer's specifications and used for cDNA synthesis. TaqMan universal PCR master mix (Applied Biosystems) was used for qPCR reactions on the MX3005P QPCR systems (Stratagene). Copies/µl were calculated using the standard curve method and MxPro software. Positive test and control samples had a Ct value <30; Ct values 30-40 are designated as weak positive whilst samples Ct values ≥40 negative. (ii) TPI: Viral RNA was extracted using the MagVet™ Universal Isolation Kit (Thermo Fisher Scientific) on a KingFisher™ Flex Robot (Life Technologies). Following RNA extraction, samples were analyzed by one-step Callahan 3D quantitative real-time RT-PCR standard protocol of the World Reference Laboratory for FMDV using serotype-specific primers targeting the 1D/2A regions[16]. Numbers of copies per microliter were calculated by using the standard-curve method and MxPro software, and samples with no fluorescence above the threshold level after 40 cycles were considered negative[16].

FMDV-specific antibody detection: The FMD-specific antibody titres in buffalo were detected by a SAT1, SAT2 and SAT3-specific liquid-phase blocking ELISA (LPBE). The assays are sufficiently specific to discriminate serological responses between serotypes [61]. They were carried out as described in the OIE Manual(53).The optical density (OD_{405nm}) was measured with a Multiskan EX. Samples with serum titres >1/16 (>1.6 log10) were considered positive.

Virus Neutralization assay: Serum samples from the animals in the experimental study were titrated by a standard virus neutralization test (VNT)[62] on porcine kidney (IB-RS2) cells and the homologous virus used to infect the animals. Neutralizing antibody titers, calculated by the Spearman-Karber method, were expressed as the average of the last dilution of serum that neutralizes the virus in 50% of the wells. VNTs were performed twice and yielded comparable results.

Ethical clearance

Ethical clearance was obtained from Oregon State University (ACUP 4478), South African National Parks (project #JOLAE 1157), the South African Department of Agriculture, Forestry and Fisheries: Directorate of Animal Health (Section 20 permit #12/11/1/8/3), Onderstepoort Veterinary Research Animal Ethics Committee (#100261Y5).

All samples collected were packaged according to the Regulations of the National Road Traffic Act, 1996 of South Africa and transported under veterinary Red Cross permits. The Pirbright Institute is the OIE and FAO World reference laboratory for FMD and regularly receives samples containing live virus from regional reference laboratories around the globe, including the ARC-Onderstepoort Veterinary Institute. All samples are sent by IATA trained staff using dedicated specialist couriers.

Supplementary Text

S1 – S5. Estimating model parameters to understand endemic persistence of FMDVs in African buffalo

S1 Duration of maternal antibodies against FMDV in African buffalo

Data from the cohort study (Fig. 1b in the main paper) were used to determine the interval when maternally-derived immunity waned in each calf for which the dam was known to have a protective titre at the time of its birth. The duration of maternal immunity was assumed to follow a gamma distribution. The likelihood for the distribution parameters (mean and shape parameter) is given by,

$$L(\theta) = \prod_j \prod_s \int_{a_0^{(j,s)}}^{a_1^{(j,s)}} f(a; k_s, \mu_s)\, \mathrm{d}a,$$

where j is an index identifying each calf, s is the serotype, a_0 and a_1 are the ages at which the last protective titre and the first non-protective titre was observed for each calf, respectively (see Fig. 1b in the main paper), and f is the probability density function for the gamma distribution with (serotype-specific) shape parameter and mean, k_s and μ_s, respectively. The gamma distribution is parameterised as,

$$f(x; k, \mu) = \frac{1}{\Gamma(k)} \frac{k}{\mu} \left(\frac{kx}{\mu} \right)^{k-1} \exp\left(-\frac{kx}{\mu} \right),$$

where $k>0$ is the shape parameter, $\mu>0$ is the mean and $\Gamma(k)$ is a gamma function. This parameterisation for the gamma distribution is used for all analyses in the study.

Two possibilities for the distribution parameters were considered. In the first, the parameters were assumed to be common to all serotypes, while in the second they were assumed to differ amongst the serotypes. In the second model, the parameters for each serotype were assumed to be drawn from higher-level gamma distributions (i.e. there is hierarchical structure in the parameters), such that $k_s \sim \text{Gamma}(a_k, m_k)$ and $\mu_s \sim \text{Gamma}(a_\mu, m_\mu)$ where m_p and a_p are the mean and shape parameter, respectively, for the hierarchical gamma distribution for parameter p (=k or μ).

Data from duration of maternal antibodies from an earlier experiment (Bengis et al. 1986) were used to construct a prior for the mean duration (exponential with mean 0.5 years). Exponential priors with mean 100 were used for the shape parameter in model 1 and for the mean and shape parameter in the hierarchical gamma distribution for the shape parameter in model 2.

Samples from the joint posterior distribution were generated using an adaptive Metropolis algorithm [63]. This was adapted to tune the scaling factor during burn-in so that the acceptance rate was between 20% and 40%, allowing for more efficient sampling of the target distribution [64]. The algorithm was implemented in Matlab (version 2019b; The Mathworks Inc.) and the code is available online[52]. Two chains of 400,000 iterations were run, with the first 200,000 iterations of each chain discarded to allow for burn-in. The chains were then thinned (taking every 20th sample) to reduce autocorrelation amongst the samples. Convergence of the scheme was assessed visually and by examining various criteria provided in the coda package [65] in R [66].

The two possibilities for the distribution parameters (i.e. common to serotypes or different amongst serotypes) were compared using the deviance information criterion (DIC) [67]. There was no evidence that the duration of maternal antibodies differed amongst serotypes (model with common parameters: DIC=217.6; model with serotype-specific parameters: DIC=216.1). The posterior estimates for the mean and shape parameters are presented in Table S1.

S2 Epidemiological parameters for African buffalo acutely infected with FMDV

S2.1 Parameter estimation

To quantify transmission of FMDVs during acute infection, the results of the experimental study were analysed using either *SIR* (susceptible (i.e. uninfected)-infected (and infectious)-recovered) or *SEIR* (susceptible-exposed (i.e. infected but not yet infectious)-infectious-recovered) models [68]. In both models, a buffalo was assumed to be infectious if FMDV RNA was detected in its blood.

The force of infection for a buffalo is given by $\lambda_s(t)=\beta_s I(t)/N(t)$ where s is the strain used in the transmission experiment (i.e. SAT-1, SAT-2 or SAT-3), $I(t)$ and $N(t)$ are the number of infectious buffalo and total number of buffalo in the pen at time t, respectively, and β_s is the strain-specific transmission rate. Where included, the latent period (i.e. the time from infection to becoming infectious) for each buffalo was assumed to be drawn from a gamma distribution with strain-specific mean $\mu_E^{(s)}$ and shape parameter $k_E^{(s)}$. Finally, the duration of the infectious period was assumed to follow a gamma distribution with strain-specific mean $\mu_I^{(s)}$ and shape parameter $k_I^{(s)}$. The basic reproduction number for strain s can be computed as $R_0^{(s)}=\beta_s\mu_I^{(s)}$.

Parameters (transmission rates, latent and infectious period parameters) were estimated in a Bayesian framework, including a data augmentation step, such that the unobserved infection times and partially observed latent and infectious periods are included in the analysis as nuisance parameters (Hu et al. 2017).

The likelihood for the data, L, can be split into two components, one relating to the inoculated buffalo, L_I, and one related to the in-contact buffalo, L_C, so that,

$$L(\boldsymbol{\varphi}, \mathbf{t_I}, \mathbf{E}, \mathbf{I}) = L_I(\boldsymbol{\varphi}, \mathbf{I}) \times L_C(\boldsymbol{\varphi}, \mathbf{t_I}, \mathbf{E}, \mathbf{I}),$$

where $\boldsymbol{\varphi}$ is a vector of model parameters and $\mathbf{t_I}=\{t_I^{(j)}\}$, $\mathbf{E}=\{E_j\}$ and $\mathbf{I}=\{I_j\}$ are vectors of infection times, latent periods and infectious periods, respectively. The likelihood for the *SIR* model is identical except that terms related to the latent periods do not need to be included.

Inoculated buffalo were assumed to be infected at t=0 and all were positive at the first observation time after inoculation (t=2). Accordingly, no inferences were drawn about the latent period for inoculated buffalo. However, the resulting uncertainty in the infectious period was incorporated in the likelihood by assuming the latent period could be between zero and two days, so that,

$$L_I(\boldsymbol{\varphi}, \mathbf{I}) = \prod_j \int_{I_j-2}^{I_j} f_I(i; k_I^{(s_j)}, \mu_I^{(s_j)})\, \mathrm{d}i,$$

where s_j is the strain with which animal j was inoculated, f_I is the probability density function (PDF) for the gamma-distributed infectious periods.

The likelihood for the in-contact buffalo is given by,

$$L_C(\boldsymbol{\varphi}, \mathbf{t_I}, \mathbf{E}, \mathbf{I}) = \prod_j \lambda_{s_j}(t_I^{(j)}; \beta_{s_j}) \exp\left(-\int_{t_0}^{t_I^{(j)}} \lambda_{s_j}(\tau; \beta_{s_j}) \, \mathrm{d}\tau \right) \times$$
$$= \prod_j f_E(E_j; k_E^{(s_j)}, \mu_E^{(s_j)}) \times$$
$$= \prod_j f_I(I_j; k_I^{(s_j)}, \mu_I^{(s_j)})^{1-c_j} \times (1 - F_I(t_{LP}^{(j)} - t_I^{(j)} - E_j; k_I^{(s_j)}, \mu_I^{(s_j)}))^{c_j}.$$

The first term in the likelihood is the probability that buffalo j becomes infected at time $t_I^{(j)}$ (conditional on not having been infected previously; t_0 is the time at which the in-contact buffalo were put in the pen). The second term corresponds to the gamma-distributed latent period for buffalo j, E_j (with PDF, f_E). The third term corresponds to the gamma-distributed infectious period for buffalo j (with PDF, f_I, and cumulative density function (CDF), F_I), where c_j is a variable indicating whether (c_j=1) or not (c_j=0) animal j was still viral RNA-positive at the final observation time. Parameters describing the infectious period (k_I, μ_I) are informed by data from both needle-inoculated and contact-challenged buffalo because transmission experiments in cattle indicate that infection route does not influence this parameter [69].

The infection times, latent periods and infectious periods for the animals were constrained so that they were consistent with the virus isolation data. In the case of the *SIR* model, the appropriate constraints are

$$t_{LN}^{(j)} < t_I^{(j)} < t_{FP}^{(j)},$$
$$t_{LP}^{(j)} < t_I^{(j)} + I_j < t_{FN}^{(j)},$$

while for the *SEIR* model, they are,

$$0 < t_I^{(j)} < t_{FP}^{(j)},$$
$$t_{LN}^{(j)} < t_I^{(j)} + E_j < t_{FP}^{(j)},$$
$$t_{LP}^{(j)} < t_I^{(j)} + E_j + I_j < t_{FN}^{(j)},$$

where *LN*, *FP*, *LP* and *FN* denote the last negative, first positive, last positive and first negative blood sample, respectively.

The results for all strains were analysed together, considering several possibilities for variation amongst strains in the transmission rate and latent and infectious period parameters (see Table S2). Where they varied amongst strains, the parameters for each strain were assumed to be drawn from higher-level exponential distributions (i.e. there is hierarchical structure in the parameters). In this case,

$$\beta_s \sim \text{Exponential}(\mu_\beta),$$
$$k_E^{(s)} \sim \text{Exponential}(\mu_{k_E}),$$
$$\mu_E^{(s)} \sim \text{Exponential}(\mu_{\mu_E}),$$
$$k_I^{(s)} \sim \text{Exponential}(\mu_{k_I}),$$
$$\mu_I^{(s)} \sim \text{Exponential}(\mu_{\mu_I}),$$

where μ_p is the mean for the hierarchical distribution for parameter p (=β, k_E, μ_E, k_I or μ_I). In total, ten models were fitted to the data: four *SIR* models and six *SEIR* models (see Table S2).

Priors were constructed for the latent and infectious period parameters based on data for the acute phase of infection for the buffalo (*16*). Specifically, an exponential prior with mean 1 was used for the shape parameter for the latent period, a gamma prior with mean 2 and shape 2 was used for the mean latent period, an exponential prior with mean 1 was used for the shape parameter for the infectious period, a gamma prior with mean 6 and shape 2 was used for the mean latent period. For the transmission parameter, a gamma prior with mean 1.85 and shape 1.39 was constructed (see section S2.2 below) based on the outcome of previous transmission experiments [22,24]. When between-strain variation (i.e. hierarchical structure) was included for a parameter, the hyperprior for the parameter mean (μ_η) was the same as the prior for that parameter without hierarchical structure.

Samples from the joint posterior distribution were generated using an adaptive Metropolis scheme as described in section S1 above, except two chains of 20,000,000 iterations were run, with the first 10,000,000 iterations of each chain discarded to allow for burn-in. The chains were then thinned by taking every 1000th sample.

Because the DIC is not uniquely defined for data augmentation models [70], the different transmission models were compared using leave-one-out (LOO) cross-validation methods [71,72]. For computational efficiency, approximate LOO was implemented using Pareto-smoothed importance sampling (PSIS) from the MCMC chains as described in Vehtari et al. (2017). In the PSIS-LOO approach, we computed -2×expected log pointwise predictive density (elpd) for a model as a measure of its predictive accuracy. (Here, multiplication by -2 puts it on the conventional scale of deviance.)

The results of model comparison are shown in Table S2 and the parameters for the selected model (*SEIR* model in which all parameters vary amongst strains) are presented in Table S1.

S2.2 Constructing the prior distribution for the acute transmission rate

Two previous experiments have considered transmission of FMDV from acutely-infected African buffalo [22,24]. For each experiment we extracted the number of inoculated buffalo, the number of in-contact buffalo, the number of these which became infected and the duration of the challenge (i.e. the time from when the in-contact animals were introduced to the inoculated ones until virus was first isolated from an in-contact animal) (see Table S3). The likelihood for the data can be written as,

$$L(\beta) = \prod_j \exp\left(-\frac{\beta I_j t_C^{(j)} n_U^{(j)}}{N_j}\right) \times \left(1 - \left(\exp\left(-\frac{\beta I_j t_C^{(j)}}{N_j}\right)\right)\right)^{n_I^{(j)}},$$

where I is the number of inoculated buffalo, t_C is the duration of challenge, n_U the number of in-contact buffalo that remain uninfected at the end of the challenge period, n_I is the number of in-contact buffalo that become infected during the challenge period and N is the total number of buffalo in the jth experiment (Table S3). The posterior distribution for the transmission rate, $p(\beta)$, is given by,

$$p(\beta) = \frac{L(\beta)\pi(\beta)}{\int_0^\infty L(b)\pi(b)\,\mathrm{d}b},$$

where $\pi(\beta)$ is the prior distribution for the transmission rate (an exponential prior with mean 100). Rather than use the full posterior, , as the prior for our analysis, we constructed a less informative prior by using a gamma distribution parameterised such that its median and interquartile range coincided with the median and 95% credible interval of the posterior distribution, . In this case, the mean is 1.85 and the shape is 1.39.

S3 Probability of a FMDV-infected buffalo becoming a carrier

The proportion of needle inoculated and contact-challenged buffalo that became carriers in the experimental study were used to estimate the probability of becoming a carrier for each strain (Table S4). Additional data on the proportion of needle inoculated buffalo that became carriers were taken from an earlier experimental study using the same three strains [16] were also included in the analysis (Table S4).

Because the carrier frequencies did not differ significantly between experiments (Fisher exact tests: SAT-1, P=1; SAT-2, P=0.82; and SAT-3, P=1), they were combined for each strain. The data were analysed using a binomial likelihood with a beta prior distribution for the probability of becoming a carrier. In this case, the posterior distribution is also a beta distribution with parameters $\alpha+C$ and $\beta+(N-C)$, where α and β are the parameters for the prior distribution and C and N are the number of carrier buffalo and the total number of acutely-infected buffalo, respectively (Table S4). A beta distribution with parameters α=1 and β=1 (i.e. a Uniform(0,1) distribution) was used as the prior for all three strains. The posterior estimates for the probabilities for each strain are presented in Table S1.

S4 Transmission rates for FMDV carrier African buffalo

S4.1 Data

To quantify transmission from carrier buffalo to naive hosts the results of the experimental study were analysed up to the first time point at which transmission was observed to have occurred (i.e. an in-contact buffalo had a positive PCR result). Where transmission of the strain did not occur, results were analysed up to the last time point when samples for both carriers of the strain were positive. In both cases this simplified the analysis by allowing us to assume the force of infection was constant during the study period. The results are summarised in Table S5 and were analysed independently for each strain, with carriers infected with other strains treated as in-contact animals.

S4.2 Parameter estimation

The likelihood for each transmission experiment is given by

$$L = {p_U}^{n_U} \times (1-(1-p_I)^{n_I}),$$

where n_U and n_I are the number of uninfected and infected in-contact buffalo at the end of the study period, respectively,

$$p_U = \exp\left(-\int_0^{t_1} \lambda(\tau)\,\mathrm{d}\tau\right),$$

$$p_I = \exp\left(-\int_0^{t_0} \lambda(\tau)\,\mathrm{d}\tau\right) \times \int_{t_0}^{t_1} \lambda(t_I) \exp\left(-\int_{t_0}^{t_I} \lambda(\tau)\,\mathrm{d}\tau\right) \mathrm{d}t_I$$

are the probabilities an in-contact buffalo remains uninfected or becomes infected during the study period, respectively, $\lambda(\tau)$ is the force of infection on day τ of the experiment, t_0 is the time of last sampling at which all in-contact buffalo were PCR-negative and t_1 is the time of first

sampling at which in-contact buffalo were PCR-positive. The term in the likelihood relating to infection of in-contact buffalo allows for the fact not all in-contact buffalo may have been infected by carriers (i.e. once the first in-contact buffalo became infected, it could transmit to other in-contact animals). Here, the force of infection is given by $\lambda(t)=\beta I(t)/N$, where I and N are the number of infectious (carrier) buffalo and total number of buffalo in the pen, respectively, and β is the transmission rate. In this case, the likelihood for those groups in which transmission occurred can be rewritten as,

$$L(\beta)=\exp\left(-\frac{2\beta t_1 n_U}{N}\right)\times\left\{1-\left[1-\left(\exp\left(-\frac{2\beta t_0}{N}\right)-\exp\left(-\frac{2\beta t_1}{N}\right)\right)\right]^{n_I}\right\},$$

while for those groups in which transmission did not occur, it can be rewritten as,

$$L(\beta)=\exp\left(-\frac{2\beta t_1 n_U}{N}\right).$$

Finally, the likelihood was constructed by multiplying the appropriate likelihoods for groups 1 and 2 and strains SAT-1, SAT-2 and SAT-3.

Two possibilities for the transmission rates were considered. In the first, the rates were assumed to be common to all strains, while in the second they were assumed to differ amongst the strains. In the second model, the rates for each strain were assumed to be drawn from a higher-level exponential distribution (i.e. there is hierarchical structure in the parameters), so that $b\sim\text{Exponential}(\mu_b)$. An exponential prior with mean 1 was assumed for the (mean) transmission rate, based on that estimated for acutely-infected buffalo (Table S1).

Samples from the joint posterior distribution were generated using an adaptive Metropolis scheme as described in section S1 above, except two chains of 300,000 iterations were run, with the first 100,000 iterations of each chain discarded to allow for burn-in. The chains were then thinned by taking every 20th sample.

The two possibilities for the transmission rates (i.e. common to strains or different amongst strains) were compared using the DIC [67]. The model in which the transmission rates differed amongst strains resulted in a significantly better fit compared to that in which the transmission rate was common (DIC=16.8 for differing rates compared with DIC=19.8 for a common rate). The posterior estimates for the transmission rates are presented in Table S1.

S5 Duration of FMDV carrier status in African buffalo

S5.1 Data

Data on virus isolation from tonsil swabs taken from eight African buffalo experimentally infected with the same three strains of FMDV (SAT-1, SAT-2 and SAT-3) as in the present study were used to estimate the duration of carrier status [16]. Only buffalo which were confirmed carriers for the strain (i.e. positive sample at 28 or more days post infection) were included in the analysis (seven for SAT-1, four for SAT-2 and five for SAT-3; one animal did not become a carrier for any of the three strains). In addition, published data for four buffalo experimentally infected with strains of SAT-2 [21,24] were used to construct a prior for the mean duration of carrier status.

Specifically, the data were used to determine the time post infection of the last positive sample for infectious FMDV and the first subsequent negative sample (Table S6). This assumes that the last positive sample was genuinely the last positive sample, but, because detection of FMDV was intermittent in all the buffalo, this may not be the case.

S5.2 Statistical methods

The duration of carrier status was assumed to follow a gamma distribution. The likelihood for the distribution parameters (mean μ and shape parameter k) is given by,

$$L = \prod_j \left(\int_{t_p^{(j)}}^{\infty} f(t;\mu_{s_j},k_{s_j})\,\mathrm{d}t \right)^{c_j} \times \left(\int_{t_p^{(j)}}^{t_n^{(j)}} f(t;\mu_{s_j},k_{s_j})\,\mathrm{d}t \right)^{1-c_j},$$

where t_p is the time of the last positive sample, t_n is the time of the first subsequent negative sample for the jth buffalo, c_j is a variable indicating whether there was (c_j=0) or was not (c_j=1) a first negative sample (i.e. whether or not the observation for the animal is right-censored) and f is the PDF for the gamma distribution and s_j is the strain with which the jth buffalo was infected.

Four possibilities for the distribution parameters were considered: (i) mean and shape parameter common to all strains; (ii) mean differs amongst strains and shape parameter common; (iii) mean common and shape parameter differs amongst strains; and (iv) mean and shape parameter differ amongst strains. Where they varied amongst strains, the parameters for each strain were assumed to be drawn from higher-level gamma distributions (i.e. there is hierarchical structure in the parameters), so that k_s~Gamma(a_k,m_k) and μ_s~Gamma(a_μ,m_μ) where m_p and a_p are the mean and shape parameter, respectively, for the hierarchical gamma distribution for parameter p.

A prior was constructed for the mean duration of carrier status using data on the duration of carrier status in experimentally-infected African buffalo (Table S6) extracted from the published literature [21,24]. Fitting an exponential distribution to these data by maximum likelihood yielded an estimate for the distribution (or hierarchical) mean of 307. Exponential priors with mean 100 were assumed for the shape parameters (distribution or hierarchical).

Samples from the joint posterior distribution were generated using an adaptive Metropolis scheme as described in section S1 above, except two chains of 300,000 iterations were run, with the first 100,000 iterations of each chain discarded to allow for burn-in. Chains were subsequently thinned by taking every 20th sample.

The four possibilities for the distribution parameters (i.e. whether the mean or shape parameter are common to strains or different amongst strains) were compared using the DIC [67]. The best-fit model was one in which the mean duration in carrier status varied amongst strains, but where the shape parameter was common to all strains (mean and shape common: DIC=76.3; mean differs, shape common: DIC=73.1; mean common, shape differs: DIC=76.2; mean and shape differ: DIC=73.3). The posterior estimates for the mean and shape parameters are presented in Table S1.

S6 Modelling FMDVs in African buffalo populations

We built a stochastic individual-based model to capture the dynamics of FMDV in African buffalo. The software we wrote to simulate and analyze the model is available for free under an open-source license (*53*). This software was written in the Python programming language (*73*).

In the model, the age and sex of each buffalo is tracked along with its immune state (Fig. S6): either immune due to maternal antibodies (M), susceptible to infection (S), exposed (E), infectious (I), carrier (C), or recovered (R). There are 7 events that can occur to each buffalo:

Death On the birth of new buffalo calf, the age at death of that calf is sampled from the mortality distribution.

Birth For each female buffalo, the time until she gives birth to a calf is sampled from its distribution. This is done when the female is herself born, to find the time until she gives birth to her first calf, and after a birth, to find the time until she gives birth to her next calf. A simple Bernoulli sample determines the sex of each calf.

Waning Each calf born to mothers who are in the recovered or carrier state is immune to infection due to maternal antibodies: at birth, the duration of maternal immunity is sampled from its distribution.

Infection For each susceptible buffalo, the time to infection is sampled from its distribution, which depends on the current number of infected buffalo in the population.

Progression On infection, the time to progression is sampled from its distribution.

Recovery On infection, the time to recovery is sampled from its distribution. A simple Bernoulli sample determines whether the recovered buffalo becomes a carrier.

Carrier recovery When a buffalo becomes a carrier, the time to recovery is sampled from its distribution.

The distributions that govern these processes are detailed below. (See also Fig. S8.) When sampling from standard distributions, we used the SciPy library (*74*). For non-standard distributions, we used the inverse transform method (*75*) for sampling.

The model simulations follow a Gillespie algorithm (*76*). For each buffalo, a list of events and the times they occur is stored. The next event over the whole population is found and the population is updated. The hazards for infection depend on the number of infectious buffalo in the population and so the times to infection are updated after each change in the population. The hazards of the other events are independent of the state of the population and so the times to these events are not updated. This process was repeated from $t = t_0$ to until there were 0 infected (exposed, infectious, and carrier) buffalo or until $t = t_0 + 10\,\mathrm{y}$. The simulations were stopped after 10 y to limit the total computation time of running many simulations.

Because we are interested in the stochastic persistence of FMDV, we initialized our simulations (i) using the stable age distribution from a deterministic model that incorporates birth seasonality; (ii) selecting the sex of each animal randomly based on equal probabilities of males and females; and (iii) finding the probabilities of being susceptible, recovered, and carrier vs. age from a simplified model with constant infection hazard fitted to a previous survey of FMDV antibodies (*78*).

For the main results (Fig. 3), we ran 1000 simulations for each model and SAT, using the posterior median values of the parameters (Table S1, Fig. 2) and an initial population of 1000 buffalo. For each model and SAT, we plotted the number of infected buffalo vs. time for each simulation, its mean over the simulations, and the distribution of simulation FMDV extinction times.

For the sensitivity analyses on population size (Fig. 4a, Fig. S1), birth seasonality (Fig. S2), and model start time (Fig. S10), we ran 1000 simulations for each model, SAT, and value of the focal parameter, using the posterior median values for the other parameters. We plotted the distribution of simulation FMDV extinction times as a function of the focal parameter and the proportion of simulations persisting 10 y as a function of the focal parameter.

In the sensitivity analysis on initial conditions (Figs. S12, S13), for each model and for the baseline parameters for each SAT, we ran 1000 simulations and using the initial conditions from each SAT. We plotted the number of infected buffalo vs. time for each simulation, its mean over the simulations, and the distribution of simulation FMDV extinction times.

For the parameter sensitivity analysis (Fig. 4b, Fig. S3), for each model and SAT, we ran a simulation with each of 20,000 samples from the posterior distributions of the parameters. From each of these simulations, we recorded the FMDV extinction time, using 10 y if FMDV persisted over the whole simulation. We calculated the partial rank correlation coefficient (PRCC; *78*, *79*) of the FMDV extinction time to the model parameters. We used our own PRCC implementation in Python that uses standard numerical libraries for rank transforming, linear regression, and calculating the Pearson correlation coefficient.

Below, we define survival and hazard functions for each event in sections S6.1–S6.7. Derivations for the stable age distribution and initial conditions are provided in sections S6.8 and S6.9. In the following, the variables t and a denote time and age, respectively.

S6.1 Death

Based on previous studies (*80*, *81*), we took the annual survival to be

$$\text{Prob}\{\text{Survival for } 1\,\text{y}\} = \begin{cases} 0.66 & \text{if } a < 1\,\text{y}, \\ 0.79 & \text{if } 1\,\text{y} \le a < 3\,\text{y}, \\ 0.88 & \text{if } 3\,\text{y} \le a < 12\,\text{y}, \\ 0.66 & \text{if } a \ge 12\,\text{y}. \end{cases} \tag{S.14}$$

Assuming that the mortality hazard is constant throughout a year gives the hazard

$$h_{\text{mortality}}(a) = -\log \text{Prob}\{\text{Survival for } 1\,\text{y}\}, \tag{S.15}$$

and the survival

$$S_{\text{mortality}}(a) = \begin{cases} 0.66^{a_\text{y}} & \text{if } a < 1\,\text{y}, \\ 0.66 \cdot 0.79^{a_\text{y}-1} & \text{if } 1\,\text{y} \le a < 3\,\text{y}, \\ 0.66 \cdot 0.79^2 \cdot 0.88^{a_\text{y}-3} & \text{if } 3\,\text{y} \le a < 12\,\text{y}, \\ 0.66 \cdot 0.79^2 \cdot 0.88^9 \cdot 0.66^{a_\text{y}-12} & \text{if } a \ge 12\,\text{y}, \end{cases} \tag{S.16}$$

with years of age $a_\text{y} = \frac{a}{1\,\text{y}}$.

S6.2 Birth

We assumed that females reach reproductive maturity at age 4 y and that the birth hazard varies at a periodic, triangular-shaped rate in time (Fig. S7).

Define the year fractional part

$$\{t\}_{\mathrm{y}} = \left\{ \frac{t}{1\,\mathrm{y}} \right\}, \tag{S.17}$$

where $\{x\}$ is the standard fractional-part function, and the year floor

$$\lfloor t \rfloor_{\mathrm{y}} = \left\lfloor \frac{t}{1\,\mathrm{y}} \right\rfloor, \tag{S.18}$$

where $\lfloor x \rfloor$ is the standard floor function. The hazard is then

$$h_{\mathrm{birth}}(t,a) = \begin{cases} 0 & \text{if } a < 4\,\mathrm{y}, \\ \mu\alpha \max\left(1 - \beta(1 - |1 - 2\{t-\tau\}_{\mathrm{y}}|), 0\right) & \text{if } a \geq 4\,\mathrm{y}, \end{cases} \tag{S.19}$$

with

$$\begin{aligned} \alpha &= \begin{cases} 1 + c_{\mathrm{v}}\sqrt{3} & \text{if } c_{\mathrm{v}} < \frac{1}{\sqrt{3}}, \\ \frac{3}{2}\left(1 + c_{\mathrm{v}}^2\right) & \text{if } c_{\mathrm{v}} \geq \frac{1}{\sqrt{3}}, \end{cases} \\ \beta &= \begin{cases} \frac{2c_{\mathrm{v}}\sqrt{3}}{1+c_{\mathrm{v}}\sqrt{3}} & \text{if } c_{\mathrm{v}} < \frac{1}{\sqrt{3}}, \\ \frac{3}{4}\left(1 + c_{\mathrm{v}}^2\right) & \text{if } c_{\mathrm{v}} \geq \frac{1}{\sqrt{3}}. \end{cases} \end{aligned} \tag{S.20}$$

The magnitude of the seasonal variation is captured by the coefficient of variation c_{v}. The time of year of the peak birth hazard is τ. The annual mean μ was determined so that the population has asymptotic growth rate $r = 0$. (See subsection S6.8.)

The cumulative hazard at time t given age a_0 at the current time t_0 is

$$H_{\mathrm{birth}}(t,t_0,a_0) = \begin{cases} 0 & \text{if } a_0 + t < 4\,\mathrm{y}, \\ \mu_{\mathrm{y}}\left(H_0 + H_1 + H_2\right) & \text{if } a_0 + t \geq 4\,\mathrm{y} \text{ and } c_{\mathrm{v}} < \frac{1}{\sqrt{3}}, \\ \mu_{\mathrm{y}}\left(H_0 + H_3 + H_4\right) & \text{if } a_0 + t \geq 4\,\mathrm{y} \text{ and } c_{\mathrm{v}} \geq \frac{1}{\sqrt{3}}, \end{cases} \tag{S.21}$$

with

$$
\begin{aligned}
\mu_{\mathrm{y}} &= \mu \cdot (1\,\mathrm{y}),\\
c &= t_0 + \max(4\,\mathrm{y} - a_0, 0\,\mathrm{y}) - \tau,\\
d &= t_0 + t - \tau,\\
H_0 &= \lfloor d \rfloor_{\mathrm{y}} - \lfloor c \rfloor_{\mathrm{y}} - 1,\\
H_1 &= \begin{cases} \frac{1}{2} + \alpha\left(\frac{1}{2} - \{c\}_{\mathrm{y}}\right)\left[1 - \beta + \beta\left(\frac{1}{2} - \{c\}_{\mathrm{y}}\right)\right] & \text{if } \{c\}_{\mathrm{y}} < \frac{1}{2},\\ \alpha\left(1 - \{c\}_{\mathrm{y}}\right)\left[1 - \beta + \beta\left(1 - \{c\}_{\mathrm{y}}\right)\right] & \text{if } \{c\}_{\mathrm{y}} \geq \frac{1}{2}, \end{cases}\\
H_2 &= \begin{cases} \alpha\{d\}_{\mathrm{y}}\left(1 - \beta\{d\}_{\mathrm{y}}\right) & \text{if } \{d\}_{\mathrm{y}} < \frac{1}{2},\\ \frac{1}{2} + \alpha\left(\{d\}_{\mathrm{y}} - \frac{1}{2}\right)\left[1 - \beta + \beta\left(\{d\}_{\mathrm{y}} - \frac{1}{2}\right)\right] & \text{if } \{d\}_{\mathrm{y}} \geq \frac{1}{2}, \end{cases}\\
H_3 &= \begin{cases} \frac{1}{2} + \alpha\beta\left(\frac{1}{2\beta} - \{c\}_{\mathrm{y}}\right)^2 & \text{if } \{c\}_{\mathrm{y}} < \frac{1}{2\beta},\\ \frac{1}{2} & \text{if } \frac{1}{2\beta} \leq \{c\}_{\mathrm{y}} < 1 - \frac{1}{2\beta},\\ \alpha\left(1 - \{c\}_{\mathrm{y}}\right)\left[1 - \beta\left(1 - \{c\}_{\mathrm{y}}\right)\right] & \text{if } \{c\}_{\mathrm{y}} \geq 1 - \frac{1}{2\beta}, \end{cases}\\
H_4 &= \begin{cases} \alpha\{d\}_{\mathrm{y}}\left[1 - \beta\{d\}_{\mathrm{y}}\right] & \text{if } \{d\}_{\mathrm{y}} < \frac{1}{2\beta},\\ \frac{1}{2} & \text{if } \frac{1}{2\beta} \leq \{d\}_{\mathrm{y}} < 1 - \frac{1}{2\beta},\\ \frac{1}{2} + \alpha\beta\left[\{d\}_{\mathrm{y}} - \left(1 - \frac{1}{2\beta}\right)\right]^2 & \text{if } \{d\}_{\mathrm{y}} \geq 1 - \frac{1}{2\beta}. \end{cases}
\end{aligned}
\tag{S.22}
$$

The survival function for t years given age a_0 at the current time t_0 is then

$$
S_{\mathrm{birth}}(t, t_0, a_0) = \exp\left(-H_{\mathrm{birth}}(t, t_0, a_0)\right). \tag{S.23}
$$

The probability density function for births time t later, given age a_0 at t_0, is

$$
f_{\mathrm{birth}}(t, t_0, a_0) = h_{\mathrm{birth}}(t_0 + t, a_0 + t) S_{\mathrm{birth}}(t, t_0, a_0). \tag{S.24}
$$

Using our birth data for 2013–2014 and 2014–2015, the maximum-likelihood estimates for the parameters of the birth hazard are coefficient of variation $c_{\mathrm{v}} = 0.613$ with peak on January 16 (0.041667 y, Fig. 1). We chose $\tau = 0$ so times are measured from the peak in the birth hazard.

At birth, a newborn is determined to be female with probability $p_{\mathrm{female}} = 0.5$ or otherwise male. A newborn has the immune state of maternal immunity if its mother was in the recovered or carrier immune states and otherwise the newborn has the susceptible immune state.

S6.3 Waning

The duration of maternal immunity was taken to be a standard gamma random variable with shape k_{waning} and mean μ_{waning}, which were estimated from our cohort study (section S1, Table S1).

S6.4 Infection

The infection hazard was taken to be

$$h_{\text{infection}}(t) = \beta_{\text{acute}} I(t) + \beta_{\text{carrier}} C(t), \tag{S.25}$$

where $I(t)$ and $C(t)$ are the total number of infectious and carrier buffalo in the herd at time t. Over periods where $I(t)$ and $C(t)$ are constant, the hazard is constant, which gives an exponential random variable. The transmission parameters β_{acute} and β_{carrier} were estimated from our transmission studies (sections S2, S4; Table S1; Fig. 2).

S6.5 Progression

The duration of the latent period was taken to be a standard gamma random variable with shape $k_{\text{progression}}$ and mean $\mu_{\text{progression}}$, which were estimated from our acute-transmission study (section S2, Table S1, Fig. 2)

S6.6 Recovery

The duration of infection was taken to be a standard gamma random variable with shape k_{recovery} and mean μ_{recovery}, which were estimated from our acute-transmission study (section S2, Table S1, Fig. 2).

On recovery, buffalo become carriers with probability p_{carrier} or otherwise are recovered, i.e. fully cleared of pathogen, which was estimated from our acute-transmission study (section S3, Table S1, Fig. 2).

S6.7 Carrier recovery

The duration of the carrier state was taken to be an exponential random variable with mean $\mu_{\text{carrier recovery}}$, which was estimated with data from a previous study (section S5, Table S1).

S6.8 Stable age distribution

Because there is no additional mortality due to the pathogen, the mean density of female buffaloes of age a satisifies the McKendrick–von Foerster partial differential equation (PDE)

$$\begin{aligned} \frac{\partial n}{\partial t}(t,a) + \frac{\partial n}{\partial a}(t,a) &= -h_{\text{death}}(a) n(t,a), \\ n(t, 0\,\text{y}) &= p_{\text{female}} \int_{0\,\text{y}}^{+\infty\,\text{y}} h_{\text{birth}}(t,a) n(t,a) \text{d}a, \\ n(t_0, a) &= n_0(a). \end{aligned} \tag{S.26}$$

where $n_0(a)$ is the initial density (*82*, pp. 159–161; *83*, pp. 353–364).

Because the birth hazard, $h_{\text{birth}}(t,a)$, is periodic with period $T = 1\,\text{y}$, we found the stable age distribution and the asymptotic population growth rate using Floquet theory (*84*). Floquet theory requires the fundamental solution $\Phi(t,a,a')$ for McKendrick–von Foerster equation (S.26), which, for each a', satisfies the same PDE and birth integral as $n(t,a)$, but with an initial condition localized to age a':

$$\begin{aligned} \frac{\partial \Phi}{\partial t}(t,a,a') + \frac{\partial \Phi}{\partial a}(t,a,a') &= -h_{\text{death}}(a) \Phi(t,a,a'), \\ \Phi(t, 0\,\text{y}, a') &= p_{\text{female}} \int_{0\,\text{y}}^{+\infty\,\text{y}} h_{\text{birth}}(t,a) \Phi(t,a,a') \text{d}a, \\ \Phi(t_0, a, a') &= \delta(a - a'), \end{aligned} \tag{S.27}$$

where $\delta(x)$ is the Dirac delta.

To solve this numerically, we used the Crank–Nicolson method on characteristics and the composite trapezoid rule for the birth integral (*85*). Given the time step Δt, let $a_i = i\Delta t$ and $a'_j = j\Delta t$ for $i, j \in \{0, 1, 2, \ldots, I-1\}$; $t^k = t_0 + k\Delta t$ for $k \in \{0, 1, \ldots, K-1\}$; and $\Phi^k_{i,j} \approx \Phi(t^k, a_i, a'_j)$. For each j and each $k \geq 1$, the Crank–Nicolson method on characteristics is

$$\frac{\Phi^k_{i,j} - \Phi^{k-1}_{i-1,j}}{\Delta t} = -h_{\text{death}}(a_{i-1/2}) \frac{\Phi^k_{i,j} + \Phi^{k-1}_{i-1,j}}{2}, \tag{S.28}$$

or

$$\Phi^k_{i,j} = \frac{1 - C_{i-1/2}}{1 + C_{i-1/2}} \Phi^{k-1}_{i-1,j}, \tag{S.29}$$

with

$$C_{i-1/2} = \frac{1}{2} h_{\text{death}}(a_{i-1/2}) \Delta t, \tag{S.30}$$

for $i \in \{1, 2, \ldots, I-2\}$. For $i = I-1$, a term was added to prevent buffaloes from aging out of this last age group:

$$\Phi^k_{I-1,j} = \frac{1 - C_{I-3/2}}{1 + C_{I-3/2}} \Phi^{k-1}_{I-2,j} + \frac{1 - C_{I-1}}{1 + C_{I-1}} \Phi^{k-1}_{I-1,j}, \tag{S.31}$$

with

$$C_{I-1} = \frac{1}{2} h_{\text{death}}(a_{I-1}) \Delta t. \tag{S.32}$$

For $i = 0$, the birth integral is given by the composite trapezoid rule,

$$\Phi^k_{0,j} = p_{\text{female}} \sum_{i=1}^{I-1} \frac{h_{\text{birth}}(t^k, a_i) \Phi^k_{i,j} + h_{\text{birth}}(t^k, a_{i-1}) \Phi^k_{i-1,j}}{2} \Delta t. \tag{S.33}$$

The initial condition is

$$\Phi^0_{i,j} = \begin{cases} 1 & \text{if } i = j, \\ 0 & \text{otherwise.} \end{cases} \tag{S.34}$$

Considering $\mathbf{\Phi}^k = [\Phi^k_{i,j}]$ as a matrix that evolves in time, the method is easily implemented with matrix algebra: the Crank–Nicolson step (S.28) is

$$\mathbf{\Phi}^k = \mathbf{M} \mathbf{\Phi}^{k-1}, \tag{S.35}$$

with the matrix $\mathbf{M} = [M_{i,j}]$ where

$$M_{i,j} = \begin{cases} \frac{1 - C_{i-1/2}}{1 + C_{i-1/2}} & \text{if } i = j + 1, \\ \frac{1 - C_{I-1}}{1 + C_{I-1}} & \text{if } i = j = I - 1, \\ 0 & \text{otherwise.} \end{cases} \tag{S.36}$$

Because the birth hazard can be decomposed into the product of a time-varying part and an age-varying part,

$$h_{\text{birth}}(t^k, a_i) = \hat{h}_{\text{birth}}(t^k) \bar{h}_{\text{birth}}(a_i), \tag{S.37}$$

the birth integral (S.33) is then

$$\mathbf{\Phi}^k_0 = \hat{h}_{\text{birth}}(t^k) \mathbf{v} \mathbf{\Phi}^k, \tag{S.38}$$

with the vector $\mathbf{v} = [v_i]$ for

$$v_i = \begin{cases} \frac{1}{2} p_{\text{female}} \bar{h}_{\text{birth}}(a_i) \Delta t & \text{if } i = 0 \text{ or } i = I - 1, \\ p_{\text{female}} \bar{h}_{\text{birth}}(a_i) \Delta t & \text{otherwise.} \end{cases} \tag{S.39}$$

The initial condition is

$$\mathbf{\Phi}^0 = \mathbf{I}, \tag{S.40}$$

where $\mathbf{I}$ is the $I \times I$ identity matrix.

Using this numerical scheme, we solved for the monodromy matrix, the fundamental solution after one period:

$$\mathbf{\Psi} = [\Psi_{i,j}] \approx [\Phi(t_0 + T, a_i, a'_j)]. \tag{S.41}$$

The monodromy matrix projects the population forward at by one period,

$$\mathbf{n}(t_0 + T) = \mathbf{\Psi} \mathbf{n}(t_0), \tag{S.42}$$

where $\mathbf{n}(t) = [n(t, a_i)]$. Using the monodromy matrix to repeatedly project the population forward gives

$$\mathbf{n}(t_0 + KT) = \mathbf{\Psi}^K \mathbf{n}(t_0) \to \rho_0^K \mathbf{w}_0 = \mathrm{e}^{rKT} \mathbf{w}_0 \tag{S.43}$$

as $K \to \infty$, where ρ_0 is the dominant eigenvalue, i.e. the eigenvalue with largest magnitude, of $\mathbf{\Psi}$; the corresponding right eigenvector $\mathbf{w}_0$ is the stable age distribution; and

$$r = \frac{1}{T} \log \rho_0 \tag{S.44}$$

is the asymptotic population growth rate.

We numerically computed the population growth rate and stable age distribution by using time step $\Delta t = 0.01\,\text{y}$, maximum age $a_{\max} = 35\,\text{y}$ (probability of survival $S_{\text{mortality}}(35\,\text{y}) \approx 10^{-5}$), finding the monodromy matrix using our Crank–Nicolson method, and then finding its dominant eigenvalue and corresponding eigenvector. We then used a root-finding algorithm to find the value of the mean birth hazard $\mu \approx 0.9379\,\text{y}^{-1}$ that gave growth rate $r = 0\,\text{y}^{-1}$ (Fig. S9). Halving the time step to $\Delta t = 0.005\,\text{y}$ gave a relative error for μ of 7×10^{-4} and doubling the maximum age to $a_{\max} = 70\,\text{y}$ gave a relative error of 5×10^{-6}.

For the initial conditions of the stochastic model, samples from the stable age distribution at growth rate $r = 0\,\text{y}$ were used to generate random ages of the buffalo present at time t_0. The random ages were sampled from the discrete ages $\mathbf{a} = [a_i] = [i\Delta t]$ with probabilities given by the dominant eigenvector $\mathbf{w}_0$ of the monodromy matrix.

S6.9 Initial conditions

The stochastic model was initiated on July 16, $t_0 = 0.5\,\mathrm{y}$ after the peak in the birth hazard, so that many susceptible young buffalo without maternal immunity were available or would soon be. The simulated extinction times of FMDV were insensitive to the choice of start time (Fig. S10). The model was initiated with 1000 buffalo. The ages of these buffalo were sampled from the stable age distribution and the sex of each buffalo was randomly sampled with probability $p_{\mathrm{female}} = 0.5$ of being female. The buffalo were then assigned to a random immune state with probabilities depending on the age of the buffalo, as described below. If there were fewer than 2 susceptible buffalo, the processes of choosing the initial population was restarted. Otherwise, 2 buffalo were randomly chosen among the susceptible buffalo with equal probabilities and these were changed to the infectious immune state.

To determine the probabilities of being in each immune state as a function of age, conditioned on the buffalo being alive at that age, we considered a simplified version of our model with the hazard of infection constant in time, with the times to progression and recovery very fast compared to the other times of the other transitions, and with all buffalo born into the maternal immunity state (Fig. S11). The probability of being in the maternal immunity state at age a, conditioned on being alive at age a, is simply the survival function for the waning process,

$$P_{\mathrm{M}}(a) = S_{\mathrm{waning}}(a). \tag{S.45}$$

To be in the susceptible state at age a, a buffalo must have undergone waning at some age a' and not yet been infected in the remaining time $a - a'$:

$$P_{\mathrm{S}}(a) = \int_0^a p_{\mathrm{waning}}(a')\mathrm{e}^{-h_{\mathrm{infection}}(a-a')}\mathrm{d}a', \tag{S.46}$$

where $p_{\mathrm{waning}}(a')$ is the probability density function for waning. To be in the carrier state at age a, a buffalo must have been infected at some age a', become carrier with probability p_{carrier}, and not yet undergone carrier recovery in the remaining time $a - a'$:

$$P_{\mathrm{C}}(a) = \int_0^a h_{\mathrm{infection}} P_{\mathrm{S}}(a') p_{\mathrm{carrier}} S_{\mathrm{carrier\ recovery}}(a - a')\mathrm{d}a', \tag{S.47}$$

where the probability of being infected at age a' is the product of $P_{\mathrm{S}}(a')$, the probability of being susceptible at age a', and the hazard of infection, $h_{\mathrm{infection}}$.

(For the model with only acute transmission, $p_{\text{carrier}} = 0$ so that $P_{\text{C}}(a) = 0$ for all a.) To be in the recovered state at age a, a buffalo must not be in any of the other states:

$$P_{\text{R}}(a) = 1 - P_{\text{M}}(a) - P_{\text{S}}(a) - P_{\text{C}}(a). \tag{S.48}$$

For a given hazard of infection, $h_{\text{infection}}$, the integrals in (S.46) and (S.47) were computed numerically using Gaussian quadrature.

We estimated the hazard of infection using survey data of buffalo antibodies to FMDV (*77*, Table S7). One of us, Dr. Jolles, reviewed this survey data and, for each SAT, classified each buffalo into the immune states present in our simplified model, both with and without the carrier state. The counts by immune state and age were then pooled across the SATs.

For our simplified model with immune states $\mathcal{X} = \{\text{M}, \text{S}, \text{C}, \text{R}\}$ and the count data $\mathbf{D} = [d_{a,X}]$ of buffalo of age a in immune state X, the likelihood function for the hazard of infection is

$$\begin{aligned} L\left(h_{\text{infection}} \middle| \mathbf{D}\right) &= \prod_{a \in \mathcal{A}} \binom{d_a}{\mathbf{d}_a} \prod_{X \in \mathcal{X}} \left[P_X(a)\right]^{d_{a,X}} \\ &\propto \prod_{a \in \mathcal{A}} \prod_{X \in \mathcal{X}} \left[P_X(a)\right]^{d_{a,X}}, \end{aligned} \tag{S.49}$$

with the multinomial coefficients

$$\binom{d_a}{\mathbf{d}_a} = \frac{d_a!}{\prod\limits_{X \in \mathcal{X}} d_{a,X}!}, \tag{S.50}$$

where the total number of buffalo of age a is

$$d_a = \sum_{X \in \mathcal{X}} d_{a,X}. \tag{S.51}$$

We took the ages of the buffalo to be the midpoints of the age intervals,

$$\mathcal{A} = \{0.5, 1.5, 2.5, 3.5, 5.5, 9\}. \tag{S.52}$$

We then found the maximum-likelihood value of $h_{\text{infection}}$ computationally.

To determine the random initial immune state of a buffalo of age a, the probabilities $P_{\text{M}}(a)$, $P_{\text{S}}(a)$, $P_{\text{C}}(a)$, and $P_{\text{R}}(a)$ of being in the immune states were computed using the maximum-likelihood value of $h_{\text{infection}}$. Using those probabilities, the buffalo was randomly assigned to one of corresponding immune states. The simulated number infected vs. time and FMDV extinction times were insensitive to differences in initial conditions between SATs (Figs. S12, S13).

Supplementary figures

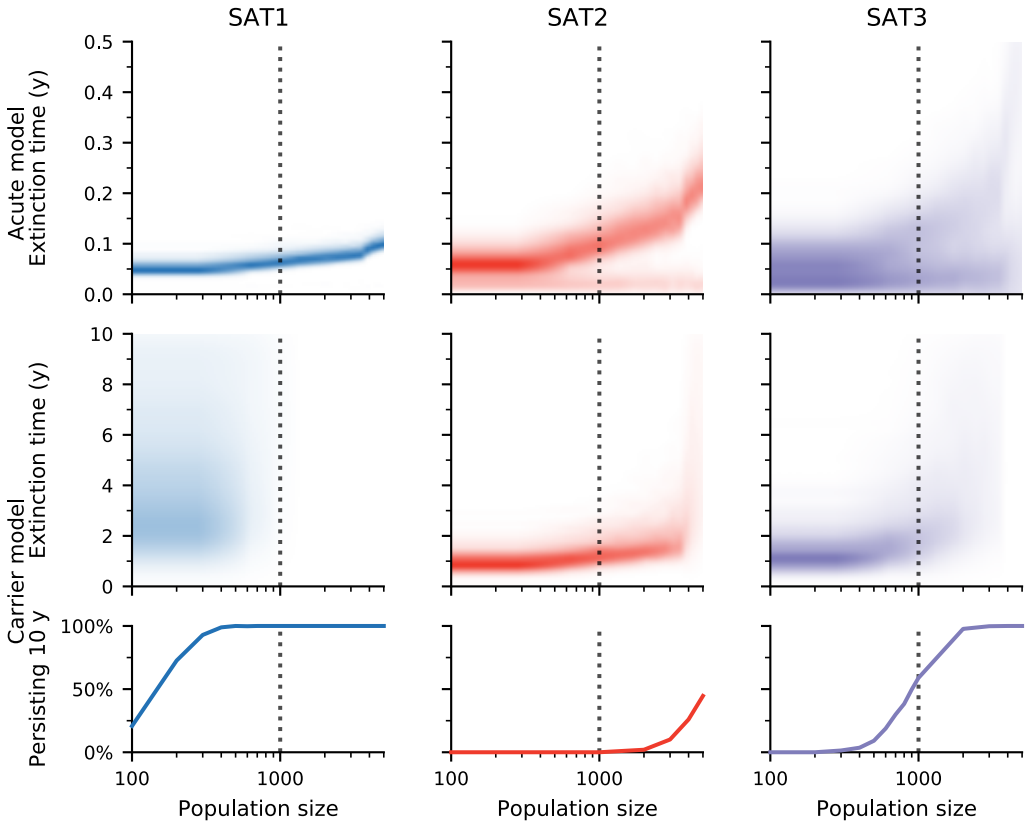

Fig. S1. The sensitivity of extinction time of FMDV to buffalo population size. For each model and each SAT, the model was simulated for 1000 runs at population sizes 100, 200, 300, 400, 500, 600, 700, 800, 900, 1000 (baseline, dotted vertical lines), 2000, 3000, 4000, and 5000. The other parameters were fixed at their baseline values. The top and middle rows of graphs show the distribution of FMDV extinction times for the model with only acute transmission and the model with both acute and carrier transmission, respectively. The bottom row shows the proportion of simulations where FMDV persisted in the buffalo population for the whole simulated 10-year period for the model with both acute and carrier transmission.

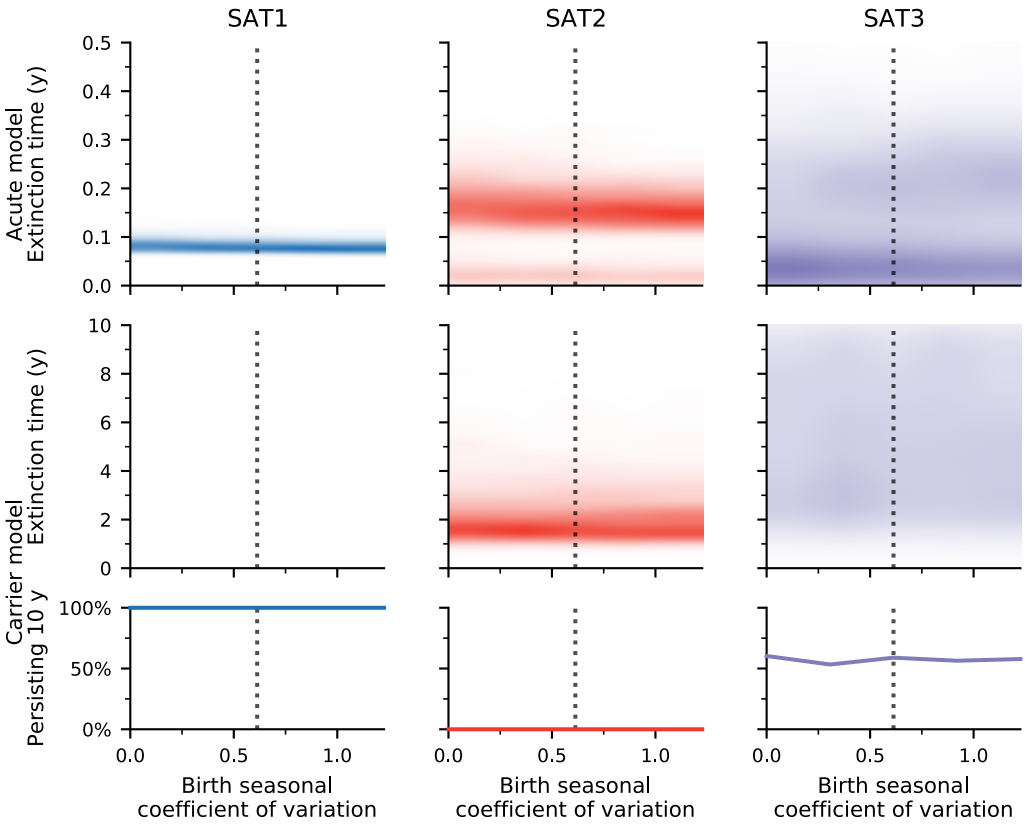

Fig. S2. The sensitivity of extinction time to birth seasonality. For each model and each SAT, the model was simulated for 1000 runs at 0, 0.5, 1 (baseline, dotted vertical lines), 1.5, and 2 times the baseline birth seasonal coefficient of variation of 0.613. The other parameters were fixed at their baseline values. The top and middle rows of graphs show the distribution of FMDV extinction times for the model with only acute transmission and the model with both acute and carrier transmission, respectively. The bottom row shows the proportion of simulations where FMDV persisted in the buffalo population for the whole simulated 10-year period with both acute and carrier transmission.

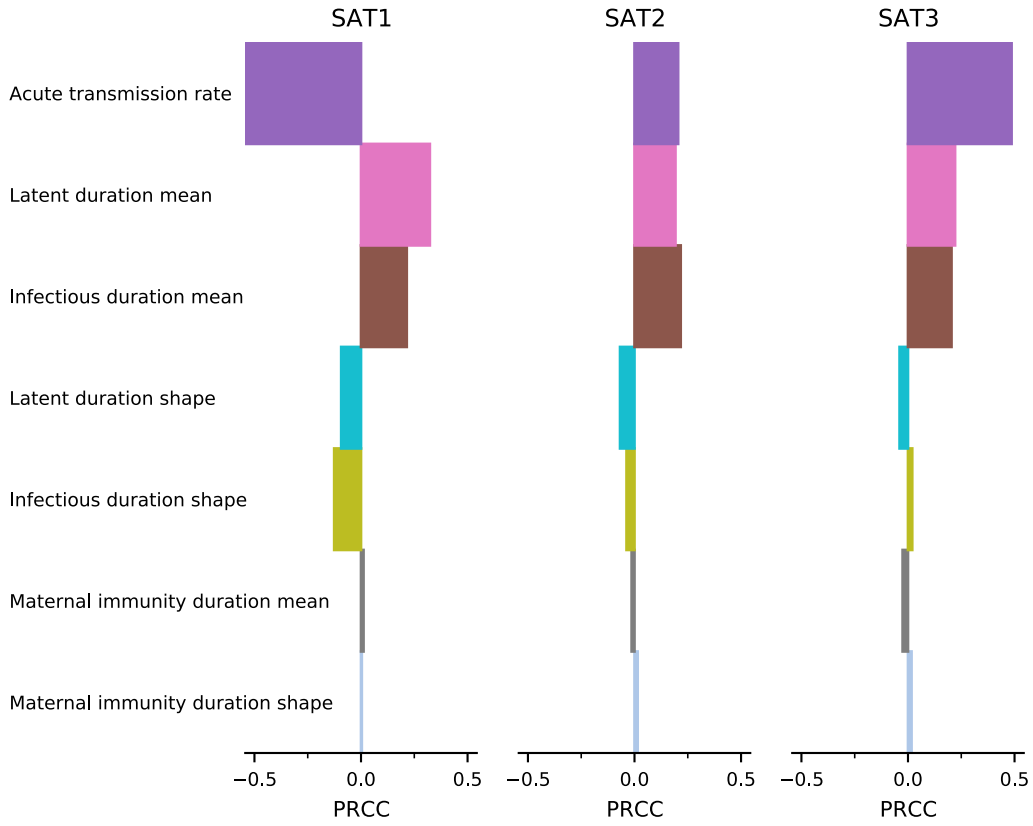

Fig. S3. The sensitivity of FMDV extinction time to model parameters, for the model with only acute transmission. The sensitivity is measured by the partial rank correlation coefficient (PRCC). The model was simulated with each of 20,000 samples from the posterior distributions of the parameters (Fig. 2, Table S1).

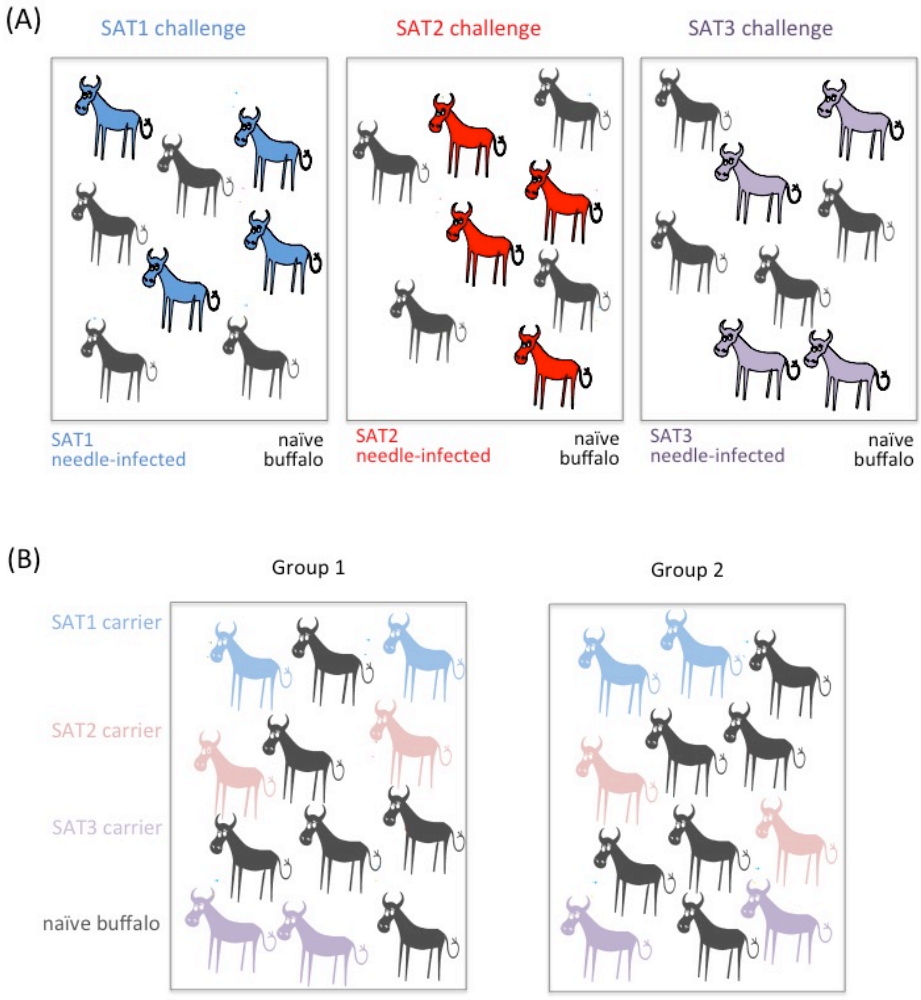

Fig. S4. Experimental design: (A) FMDV transmission during acute infection. In separate corrals for each serotype (SAT1, SAT2, SAT3), four needle-infected animals were mixed with four naïve buffalo, two days after the initial infectious challenges (needle infections). Presence of virus and antibodies to FMDVs were tested in the recipient animals on days 2, 4, 6, 8, 11, 14 and 30 post exposure to the needle infected buffalo. (B) Transmission from FMDV carriers. FMDV carrier status is defined as retention of FMDV for more than 30 days after primary infection. In two separate corrals, two groups of six carrier animals, including two per serotype, were mixed with two groups naïve animals at day 45 post-infection. Buffalo were sampled to test for FMDV transmission after two weeks post-contact, and then monthly for six months.

			Day 30 post-infection			Day 60 - 2 weeks postcontact			Day 90 - 6 weeks postcontact			Day 150 - 3.5 months			Day 180 - 4.5 months			Day 240 - 6.5 months		
	ID	Group	SAT1	SAT2	SAT3	SAT1	SAT2	SAT3	SAT1	SAT2	SAT3	SAT1	SAT2	SAT3	SAT1	SAT2	SAT3	SAT1	SAT2	SAT3
Group 1	11	SAT1	6.6	0	0	5.72	0	0.33	3.61	0	5.96	pos	0	pos	pos	0	pos	0	0	4.48
	33	SAT1	6.3	0	0	5.60	0	0	5.76	0	0	pos	0	0	pos	0	0	0	0	0
	8	SAT2	0	4.9	0	4.92	3.00	6.12	2.28	4.13	6.01	pos	0	pos	pos	0	pos	0	0	0
	28	SAT2	0	3.02	0	6.26	2.52	0.0	5.78	0.00	0	pos	0	0	pos	0	0	0	0	1.32
	26	SAT3	0	0	5.7	0	0	5.10	5.91	0	3.07	pos	0	0	pos	0	0	3.40	0	0
	35	SAT3	0	0	6.1	0	0	6.04	0	0	5.80	0	0	pos	0	0	pos	0	0	0
	1	naïve	0	0	0	3.39	0	0	4.40	0	0	pos	0	0	pos	0	0	0	0	0
	3	naïve	0	0	0	4.38	0	0	6.12	0	0	pos	0	0	pos	0	0	2.19	0	0
	18	naïve	0	0	0	0	0	4.94	0	0	5.65	0	0	pos	0	0	pos	0	0	2.19
	21	naïve	0	0	0	5.03	0	0	3.36	0	5.11	pos	0	pos	pos	0	pos	5.06	0	5.50
	30	naïve	0	0	0	4.14	0	0	6.16	0	0	pos	0	0	pos	0	0	5.83	0	0
	31	naïve	0	0	0	5.63	0	0	5.25	0	0	pos	0	0	pos	0	0	0	0	0
Group 2	7	SAT1	6.2	0	0	5.51	0	0	6.05	0	0	pos	0	0	pos	0	0	5.07	0	0
	13	SAT1	5.6	0	0	4.66	0	0	4.09	0	0	0	0	0	0	0	0	0	0	0
	20	SAT2	0	3.37	0	0	5.71	0	0	5.50	0	pos	pos	0	pos	0	0	4.31	0	0
	32	SAT2	0	5.6	0	0	3.67	0	0	4.86	0	0	pos	0	0	pos	0	0	0	0
	27	SAT3	0	0	4.5	0	0	4.59	0	0	4.89	0	0	pos	pos	0	0	5.75	0	0
	34	SAT3	0	0	4.5	0	0	4.96	6.46	0	2.52	pos	0	0	pos	0	0	0	0	0
	14	naive	0	0	0	0	0	0	5.04	0	0	pos	0	0	pos	0	0	1.04	0	0
	23	naive	0	0	0	0	0	0	5.77	0	0	pos	0	0	pos	0	0	5.77	0	0
	24	naive	0	0	0	0	0	0	7.28	0	0	pos	0	0	pos	0	0	4.42	0	0
	25	naive	0	0	0	0	0	0	6.39	0	0	pos	0	0	pos	0	0	0	0	0
	36	naive	0	0	0	0	0	0	6.71	0	0	pos	0	0	pos	0	0	5.96	0	0

Fig. S5. FMDV transmission events from carrier to naïve buffalo. Carrier buffalo are shown in blue (SAT 1), red (SAT 2) and purple (SAT 3). Lighter shades indicate loss of carrier status in these individuals. Yellow shading demarks new infections that occurred during the experimental period. The numbers are the log10 titre of virus genome per µl of sample using specific primers for each serotype (methods and results described in *16*). Samples categorized as positive (pos) were RT PCR positive but the Ct value was above a cut off of 32 (*16*). Carrier status was confirmed on day 30 post-infection. Experimental groups, each including two carriers of each serotype and six naïve buffalo, were assembled on day 46. All buffalo were sampled for FMDV testing 2 weeks post-contact, and subsequently monthly for 6 months. Samples from day 120 and day 210 have not been analyzed and are not shown here. By two weeks post-contact, at least one transmission event from a SAT1 carrier and one from a SAT3 carrier had occurred in group one, and by 6 weeks post-contact at least one more transmission event from a SAT1 carrier had occurred in group 2. Additional transmission events may have originated from carriers or may reflect secondary infections within each group.

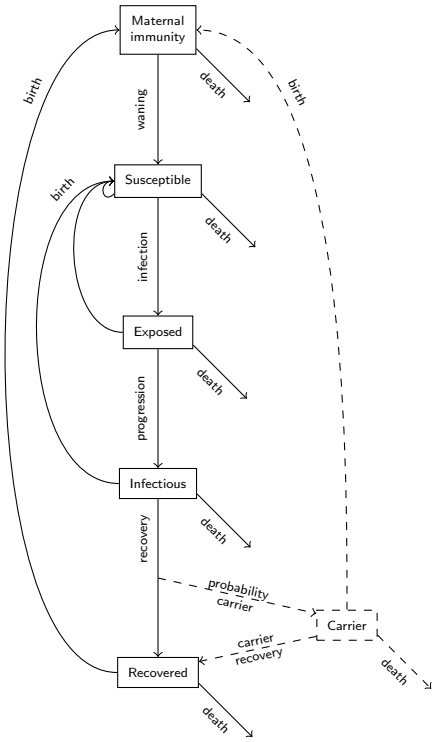

Fig. S6. Model diagram. The dashed box and arrows show the state and transitions present in the model with both acute and carrier transmission that are not present in the model with only acute transmission.

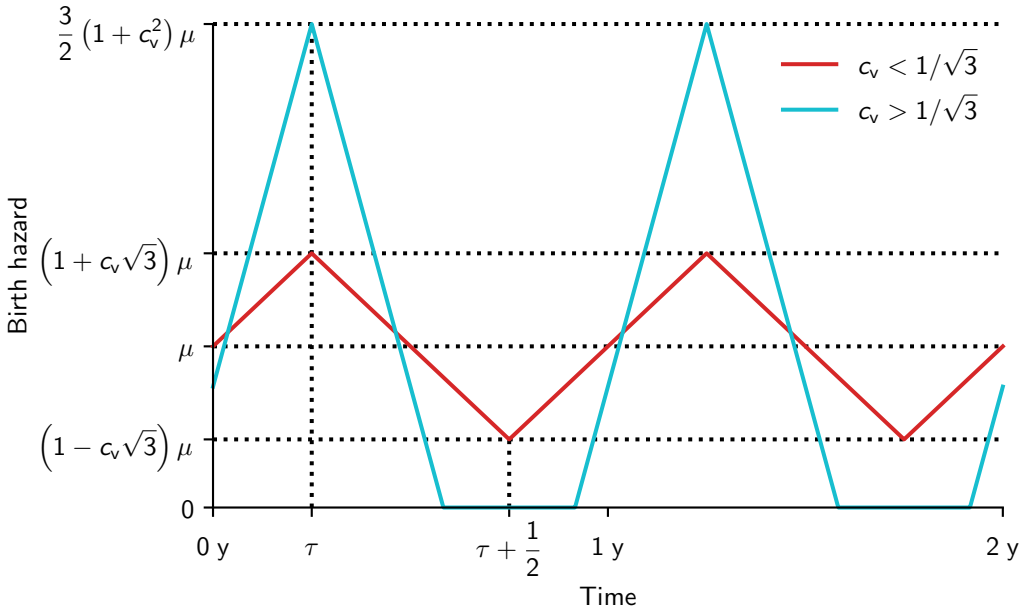

Fig. S7. Model birth hazards for ages 4 y and older.

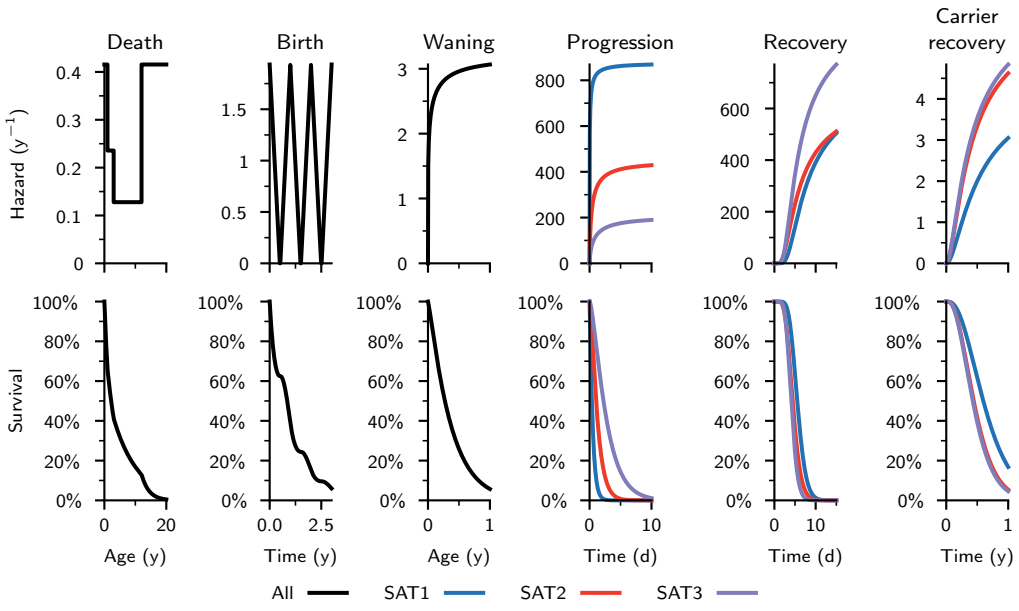

Fig. S8. Hazards and survivals for the model events.

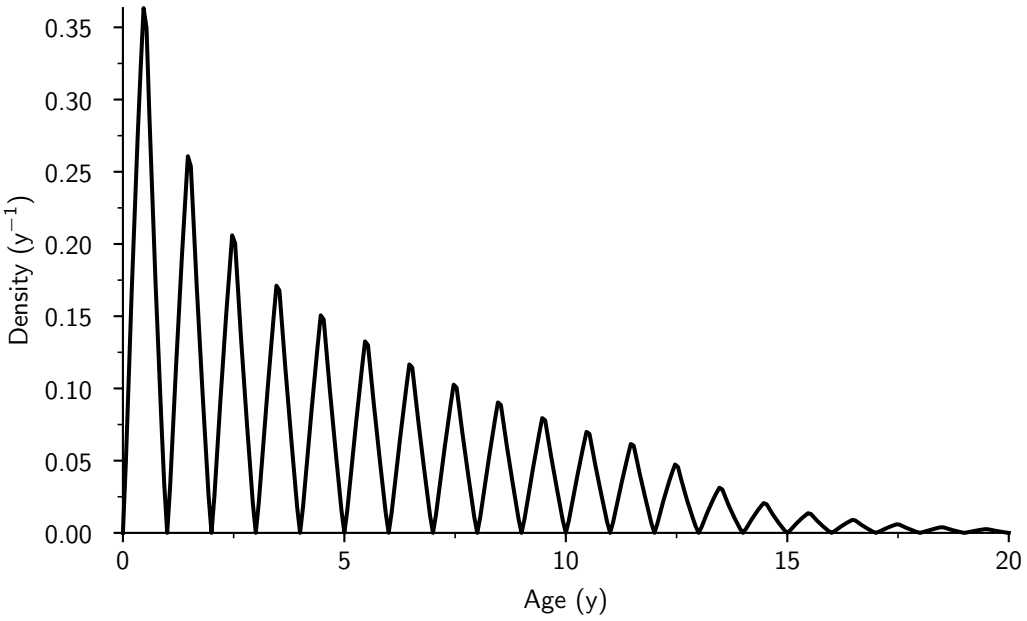

Fig. S9. The stable age distribution of the buffalo population on July 16, $t_0 = 0.5\,\mathrm{y}$ after the peak in the birth hazard.

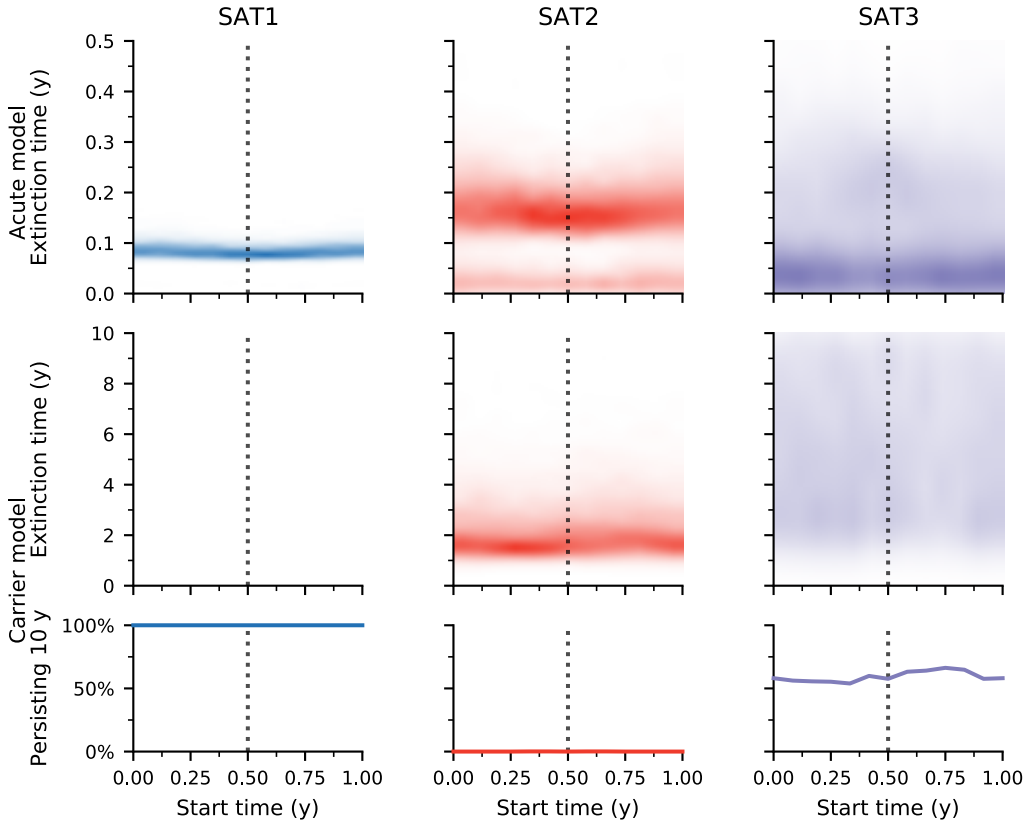

Fig. S10. The sensitivity of extinction time to model start time. For each model and each SAT, the model was simulated for 1000 runs starting $t_0 = i/12\,\mathrm{y}$ after the peak in the birth hazard, for $i = 0, 1, \ldots, 11$. The baseline value is $t_0 = 0.5\,\mathrm{y}$ (dotted vertical lines). The other parameters were fixed at their baseline values. The top and middle rows of graphs show the distribution of FMDV extinction times for the model with only acute transmission and the model with both acute and carrier transmission, respectively. The bottom row shows the proportion of simulations where FMDV persisted in the buffalo population for the whole simulated 10-year period with both acute and carrier transmission.

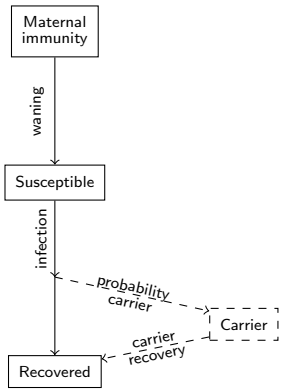

Fig. S11. Diagram of the simplified model used in finding initial conditions for the full model. The dashed box and arrows show the state and transitions present in the model with both acute and carrier transmission that are not present in the model with only acute transmission.

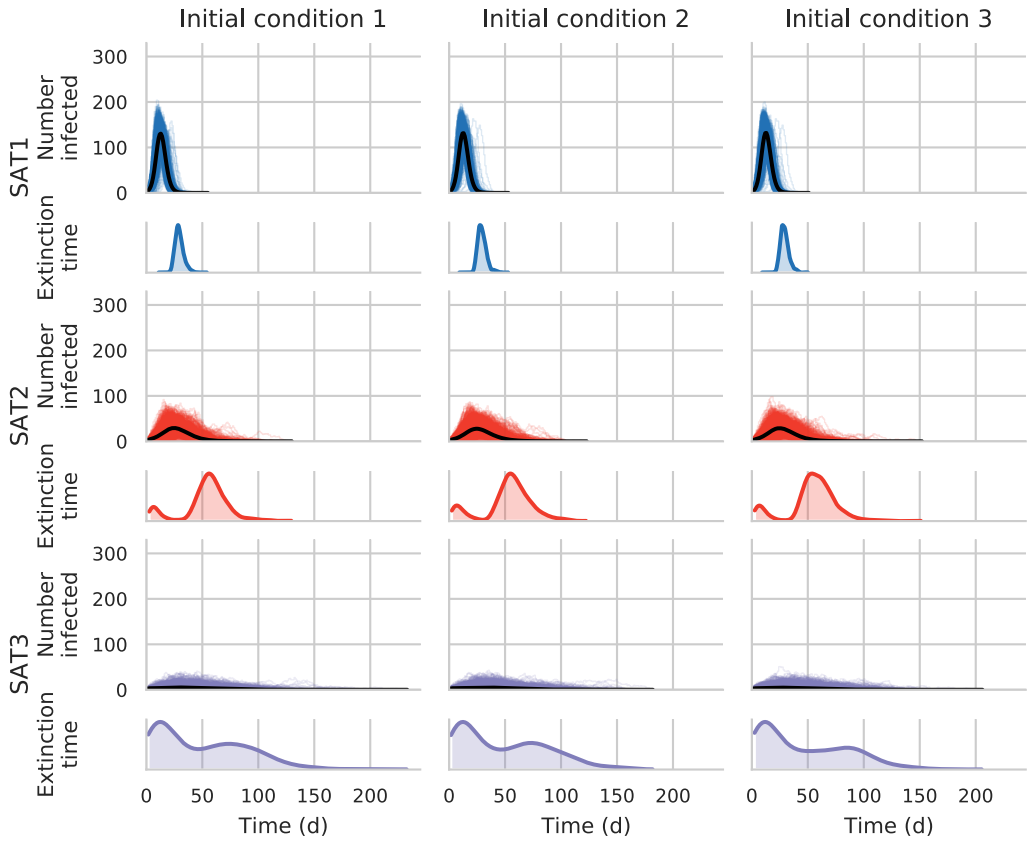

Fig. S12. The sensitivity of extinction time to initial conditions for the model with acute transmission only. For each SAT (rows of paired graphs of number infected and extinction time), the model was simulated for 1000 runs using baseline and alternate initial conditions for each SAT (columns; section S6.9). The other parameters were fixed at their baseline values. In the graphs of number infected, the thin colored curves show the number infected vs. time for the individual simulations, while the thick black curve is the mean over the simulations of the number infected vs. time. The graphs of FMDV extinction time show the distribution of extinction times (when the number infected first becomes 0) over the simulations.

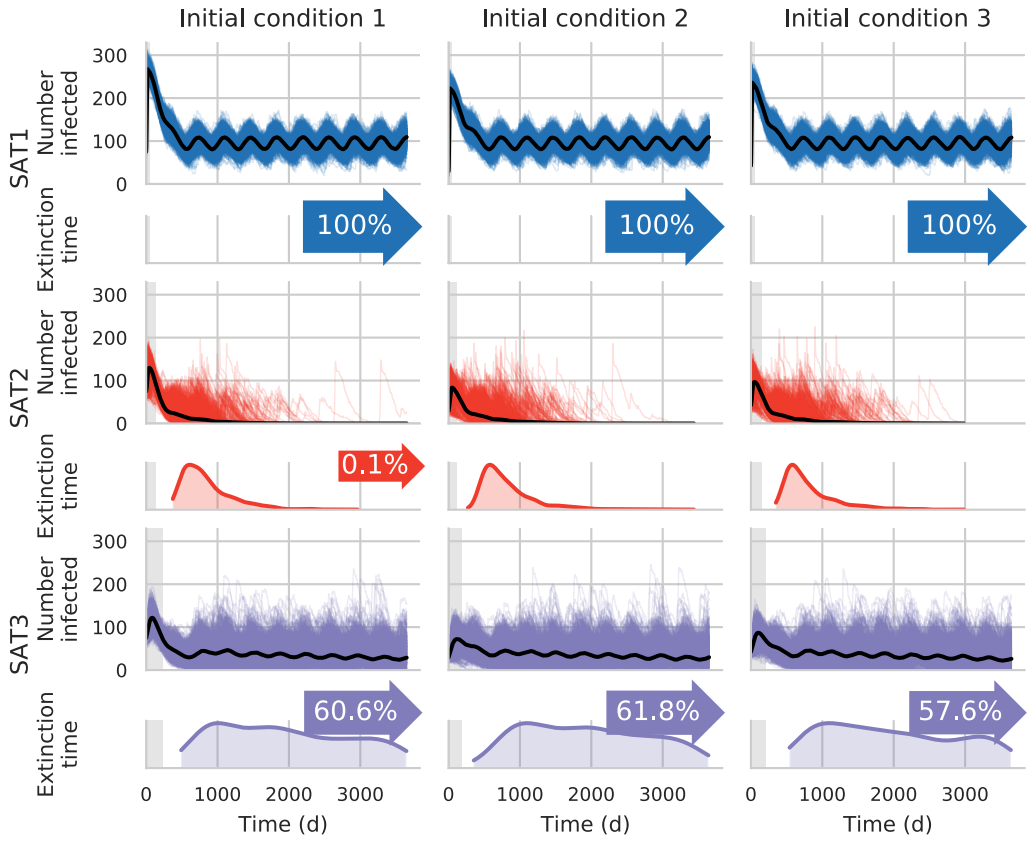

Fig. S13. The sensitivity of extinction time to initial conditions for the model with transmission from acutely infected and carrier hosts. For each SAT (rows of paired graphs of number infected and extinction time), the model was simulated for 1000 runs using baseline and alternate initial conditions for each SAT (columns; section S6.9). The other parameters were fixed at their baseline values. In the graphs of number infected, the thin colored curves show the number infected vs. time for the individual simulations, while the thick black curve is the mean over the simulations of the number infected vs. time. The graphs of FMDV extinction time show the distribution of extinction times (when the number infected first becomes 0) over the simulations, arrows show the proportion of simulations that persisted longer than 10 years, and the gray boxes show the longest persistence time for the model with acute transmission only to highlight the difference in scale.

Supplementary Tables

parameter	SAT-1	SAT-2	SAT-3
duration of maternal antibodies			
shape parameter‡		1.2 (0.8, 1.8)	
mean (years)‡		0.4 (0.3, 0.5)	
acute infection			
latent period			
shape parameter	1.2 (0.1, 8.7)	1.6 (0.2, 9.2)	1.6 (0.2, 8.3)
mean (days)	0.5 (0.02, 2.4)	1.3 (0.1, 3.5)	2.8 (0.5, 7.0)
infectious period			
shape parameter	11.8 (3.5, 33.5)	8.7 (2.4, 27.0)	11.8 (3.3, 35.3)
mean (days)	5.7 (4.4, 7.4)	4.6 (3.5, 6.3)	4.2 (3.2, 5.8)
transmission rate (per day)	2.8 (0.8, 11.3)	1.6 (0.4, 9.0)	1.2 (0.3, 7.8)
carrier infection			
probability of becoming a carrier	0.90 (0.70, 0.98)	0.44 (0.23, 0.67)	0.67 (0.44, 0.86)
duration of carrier state			
shape parameter‡		3.2 (1.3, 8.5)	
mean (days)	243 (170, 370)	180 (106, 316)	174 (104, 298)
transmission rate (per day)	0.028 (0.005, 0.10)	0.003 (0, 0.016)	0.012 (0.002, 0.04)
basic reproduction number			
acute	15.8 (4.1, 65.6)	7.5 (1.9, 41.5)	5.2 (1.3, 34.1)
carrier	6.7 (1.1, 25.1)	0.5 (0.02, 3.1)	2.1 (0.3, 8.6)
both combined	23.8 (8.2, 73.3)	7.8 (2.1, 41.7)	7.2 (2.3, 36.1)

† posterior median (95% credible interval)
‡ parameter common to all strains

Table S1. Parameters† for FMDVs in African buffalo.

model	parameters†			-2×elpd‡
	latent period	infectious period	transmission rate	
SIR				
1	none	common	common	139.6
2	none	common	varies	138.1
3	none	varies	common	135.2
4	none	varies	varies	133.4
SEIR				
5	common	common	common	138.5
6	common	common	varies	134.1
7	varies	common	common	130.2
8	common	varies	common	135.4
9	varies	varies	common	126.7
10	varies	varies	varies	126.1

† "common": common to all strains; "varies": varies amongst strains
‡ elpd: expected log pointwise predictive density

Table S2. Comparison of models for the transmission of foot-and-mouth disease virus strains in acutely-infected African buffalo.

	Gainaru et al. (*22*)		Vosloo et al. (*24*)	
serotype*	SAT-1	SAT-2	SAT-2	SAT-2
number of challenge buffalo	2	2	2	2
number of in-contact buffalo				
infected	4	4	4	1
total	4	4	4	2
duration of challenge (days)	4	4	4	7

* note: these are not the same strains as used in the present study

Table S3. Outcome of previous transmission experiments for FMDV in acutely-infected buffalo.

study	strain					
	SAT-1		SAT-2		SAT-3	
	C†	N‡	C	N	C	N
present study						
needle inoculated	4	4	2	4	3	4
contact challenged	3	3	1	4	3	4
Maree et al. (*16*)¶	7	8	4	8	5	8

† number of buffalo becoming carriers
‡ number of buffalo infected
¶ animals were co-infected with all three strains

Table S4. Number of African buffalo becoming carriers following infection with three strains of foot-and-mouth disease virus.

strain	group	N	t_0	t_1	n_U	n_I
SAT-1	1	12	0	14	3	7
	2	11	14	44	3	6
SAT-2	1	12	-	14	10	0
	2	11	-	104	9	0
SAT-3	1	12	0	14	7	3
	2	11	-	44	9	0

N - number of buffalo in the group (i.e. carrier and in-contact)

t_0 - time of last sampling at which all in-contact buffalo were PCR-negative (if transmission occurred)

t_1 - time of first sampling at which in-contact buffalo were PCR-positive (if transmission occurred) or time of last sampling at which both carriers were positive (if transmission did not occur).

n_U - number of uninfected in-contact buffalo at t_1

n_I - number of infected in-contact buffalo at t_1

Table S5. Outcome of experiments on the transmission for foot-and-mouth disease virus from carrier African buffalo.

reference	strain/serotype					
	SAT-1		SAT-2		SAT-3	
	t_{lp}†	t_{fn}‡	t_{lp}	t_{fn}	t_{lp}	t_{fn}
Maree et al. (*16*)§	316	336	136	155	126	136
	>185	-	>185	-	>185	-
	>400	-	nc¶	nc	95	109
	200	214	35	80	nc	nc
	>185	-	nc	nc	109	126
	168	185	nc	nc	nc	nc
	214	231	35	80	35	80
Dawe et al. (*21*)	-	-	126	154	-	-
	-	-	>188	-	-	-
Vosloo et al. (*24*)	-	-	366	399	-	-
	-	-	nc	nc	-	-

† t_{lp} - time of last positive virus isolation (a > sign indicates the observation is right-censored)
‡ t_{fn} - time of first subsequent negative virus isolation
¶ nc - not a carrier (i.e. no positive samples 28 days or more post infection)
§ animals were co-infected with all three strains

Table S6. Duration (in days post infection) of foot-and-mouth disease virus carrier state in African buffalo

Model	Immune state	Age (y)					
		0–1	**1–2**	**2–3**	**3–4**	**4–7**	**7–11**
Acute	Maternal immunity	17	0	0	0	0	0
	Susceptible	1	6	4	2	3	3
	Recovered	0	18	23	22	30	54
Carrier	Maternal immunity	17	0	0	0	0	0
	Susceptible	1	2	4	2	3	3
	Carrier	0	8	12	8	6	8
	Recovered	0	14	11	14	24	46

Table S7. Counts of buffalo by immune state and age, based on a survey of FMDV antibodies (*77*). The surveyed buffalo were classified by expert opinion into the immune states present in our simplified model with only acute transmission ("Acute") and to those present in our simplified model with both acute and carrier transmission ("Carrier"). These counts were then pooled across SATs. See section S6.9 for more information.

References and Notes

1. S. S. Morse, J. A. K. Mazet, M. Woolhouse, C. R. Parrish, D. Carroll, W. B. Karesh, C. Zambrana-Torrelio, W. I. Lipkin, P. Daszak, Prediction and prevention of the next pandemic zoonosis. Lancet 380, 1956–1965 (2012). doi:10.1016/S0140-6736(12)61684-5 Medline

2. D. J. Paton, S. Gubbins, D. P. King, Understanding the transmission of foot-and-mouth disease virus at different scales. Curr. Opin. Virol. 28, 85–91 (2018). doi:10.1016/j.coviro.2017.11.013 Medline

3. R. Marguta, A. Parisi, Periodicity, synchronization and persistence in pre-vaccination measles. J. R. Soc. Interface 13, 20160258 (2016). doi:10.1098/rsif.2016.0258 Medline

4. M. Domenech de Cellès, F. M. G. Magpantay, A. A. King, P. Rohani, The pertussis enigma: Reconciling epidemiology, immunology and evolution. Proc. R. Soc. B 283, 20152309 (2016). doi:10.1098/rspb.2015.2309 Medline

5. A. J. Peel, J. R. C. Pulliam, A. D. Luis, R. K. Plowright, T. J. O'Shea, D. T. S. Hayman, J. L. N. Wood, C. T. Webb, O. Restif, The effect of seasonal birth pulses on pathogen persistence in wild mammal populations. Proc. R. Soc. B 281, 20132962 (2014). doi:10.1098/rspb.2013.2962 Medline

6. M. J. Keeling, M. E. Woolhouse, D. J. Shaw, L. Matthews, M. Chase-Topping, D. T. Haydon, S. J. Cornell, J. Kappey, J. Wilesmith, B. T. Grenfell, Dynamics of the 2001 UK foot and mouth epidemic: Stochastic dispersal in a heterogeneous landscape. Science 294, 813–817 (2001). doi:10.1126/science.1065973 Medline

7. I. Chis Ster, P. J. Dodd, N. M. Ferguson, Within-farm transmission dynamics of foot and mouth disease as revealed by the 2001 epidemic in Great Britain. Epidemics 4, 158–169 (2012). doi:10.1016/j.epidem.2012.07.002 Medline

8. G. R. Thomson, W. Vosloo, J. J. Esterhuysen, J. Schlundt, Maintenance of foot and mouth disease viruses in buffalo (Syncerus caffer Sparrman, 1779) in southern Africa. Rev. Sci. Tech. 11, 1097–1107 (1992). doi:10.20506/rst.11.4.646 Medline

9. J. A. W. Coetzer, G. R. Thomson, R. C. Tustin, Infectious Diseases of Livestock: With Special Reference to Southern Africa (Oxford Univ. Press, 1994).

10. D. J. Paton, K. J. Sumption, B. Charleston, Options for control of foot-and-mouth disease: Knowledge, capability and policy. Philos. Trans. R. Soc. B 364, 2657–2667 (2009). doi:10.1098/rstb.2009.0100 Medline

11. M. Casey-Bryars, R. Reeve, U. Bastola, N. J. Knowles, H. Auty, K. Bachanek-Bankowska, V. L. Fowler, R. Fyumagwa, R. Kazwala, T. Kibona, A. King, D. P. King, F. Lankester, A. B. Ludi, A. Lugelo, F. F. Maree, D. Mshanga, G. Ndhlovu, K. Parekh, D. J. Paton, B. Perry, J. Wadsworth, S. Parida, D. T. Haydon, T. L. Marsh, S. Cleaveland, T. Lembo, Waves of endemic foot-and-mouth disease in eastern Africa suggest feasibility of proactive vaccination approaches. Nat. Ecol. Evol. 2, 1449–1457 (2018). doi:10.1038/s41559-018-0636-x Medline

12. T. J. D. Knight-Jones, J. Rushton, The economic impacts of foot and mouth disease - what

are they, how big are they and where do they occur? Prev. Vet. Med. 112, 161–173 (2013). doi:10.1016/j.prevetmed.2013.07.013 Medline

13. P. S. Dawe, F. O. Flanagan, R. L. Madekurozwa, K. J. Sorensen, E. C. Anderson, C. M. Foggin, N. P. Ferris, N. J. Knowles, Natural transmission of foot-and-mouth disease virus from African buffalo (Syncerus caffer) to cattle in a wildlife area of Zimbabwe. Vet. Rec. 134, 230–232 (1994). doi:10.1136/vr.134.10.230 Medline

14. G. Omondi, M. A. Alkhamis, V. Obanda, F. Gakuya, A. Sangula, S. Pauszek, A. Perez, S. Ngulu, R. van Aardt, J. Arzt, K. VanderWaal, Phylogeographical and cross-species transmission dynamics of SAT1 and SAT2 foot-and-mouth disease virus in Eastern Africa. Mol. Ecol. 28, 2903–2916 (2019). doi:10.1111/mec.15125 Medline

15. J. B. Condy, R. S. Hedger, Experiences in the establishment of a herd of foot -and-mouth disease free African buffalo (Syncerus caffer). S. Afr. J. Wildl. Res. 8, 87–89 (1978).

16. F. Maree, L.-M. de Klerk-Lorist, S. Gubbins, F. Zhang, J. Seago, E. Pérez-Martín, L. Reid, K. Scott, L. van Schalkwyk, R. Bengis, B. Charleston, N. Juleff, Differential Persistence of Foot-and-Mouth Disease Virus in African Buffalo Is Related to Virus Virulence. J. Virol. 90, 5132–5140 (2016). doi:10.1128/JVI.00166-16 Medline

17. J. B. Condy, R. S. Hedger, C. Hamblin, I. T. Barnett, The duration of the foot-and-mouth disease virus carrier state in African buffalo (i) in the individual animal and (ii) in a free-living herd. Comp. Immunol. Microbiol. Infect. Dis. 8, 259–265 (1985). doi:10.1016/0147-9571(85)90004-9 Medline

18. E. C. Anderson, W. J. Doughty, J. Anderson, R. Paling, The pathogenesis of foot-and-mouth disease in the African buffalo (Syncerus caffer) and the role of this species in the epidemiology of the disease in Kenya. J. Comp. Pathol. 89, 541–549 (1979). doi:10.1016/0021-9975(79)90045-8 Medline

19. R. G. Bengis, G. R. Thomson, R. S. Hedger, V. De Vos, A. Pini, Foot-and-mouth disease and the African buffalo (Syncerus caffer). 1. Carriers as a source of infection for cattle. Onderstepoort J. Vet. Res. 53, 69–73 (1986). Medline

20. J. B. Condy, R. S. Hedger, The survival of foot-and-mouth disease virus in African buffalo with non-transference of infection to domestic cattle. Res. Vet. Sci. 16, 182–185 (1974). doi:10.1016/S0034-5288(18)33749-4 Medline

21. P. S. Dawe, K. Sorensen, N. P. Ferris, I. T. Barnett, R. M. Armstrong, N. J. Knowles, Experimental transmission of foot-and-mouth disease virus from carrier African buffalo (Syncerus caffer) to cattle in Zimbabwe. Vet. Rec. 134, 211–215 (1994). doi:10.1136/vr.134.9.211 Medline

22. M. D. Gainaru, G. R. Thomson, R. G. Bengis, J. J. Esterhuysen, W. Bruce, A. Pini, Foot-and-mouth disease and the African buffalo (Syncerus caffer). II. Virus excretion and transmission during acute infection. Onderstepoort J. Vet. Res. 53, 75–85 (1986). Medline

23. R. S. Hedger, J. B. Condy, Transmission of foot-and-mouth disease from African buffalo virus carriers to bovines. Vet. Rec. 117, 205 (1985). doi:10.1136/vr.117.9.205-a Medline

24. W. Vosloo, A. D. Bastos, E. Kirkbride, J. J. Esterhuysen, D. J. van Rensburg, R. G. Bengis,

D. W. Keet, G. R. Thomson, Persistent infection of African buffalo (Syncerus caffer) with SAT-type foot-and-mouth disease viruses: Rate of fixation of mutations, antigenic change and interspecies transmission. J. Gen. Virol. 77, 1457–1467 (1996). doi:10.1099/0022-1317-77-7-1457 Medline

25. C. Stenfeldt, J. Arzt, The Carrier Conundrum; A Review of Recent Advances and Persistent Gaps Regarding the Carrier State of Foot-and-Mouth Disease Virus. Pathogens 9, 167 (2020). doi:10.3390/pathogens9030167 Medline

26. Materials and methods are available as supplementary materials.

27. P. C. Cross, D. M. Heisey, J. A. Bowers, C. T. Hay, J. Wolhuter, P. Buss, M. Hofmeyr, A. L. Michel, R. G. Bengis, T. L. F. Bird, J. T. Du Toit, W. M. Getz, Disease, predation and demography: Assessing the impacts of bovine tuberculosis on African buffalo by monitoring at individual and population levels. J. Appl. Ecol. 46, 467–475 (2009). doi:10.1111/j.1365-2664.2008.01589.x

28. E. E. Gorsich, R. S. Etienne, J. Medlock, B. R. Beechler, J. M. Spaan, R. S. Spaan, V. O. Ezenwa, A. E. Jolles, Opposite outcomes of coinfection at individual and population scales. Proc. Natl. Acad. Sci. U.S.A. 115, 7545–7550 (2018). doi:10.1073/pnas.1801095115 Medline

29. B. S. Dugovich, Investigating Variation in Immunity and Infection Risk in Wild Ungulates (Oregon State Univ., 2019).

30. J. Domenech, J. Lubroth, K. Sumption, Immune protection in animals: The examples of rinderpest and foot-and-mouth disease. J. Comp. Pathol. 142 (suppl. 1), S120–S124 (2010). doi:10.1016/j.jcpa.2009.11.003 Medline

31. R. J. Nelson, Seasonal immune function and sickness responses. Trends Immunol. 25, 187–192 (2004). doi:10.1016/j.it.2004.02.001 Medline

32. R. J. Orton, C. F. Wright, M. J. Morelli, N. Juleff, G. Thébaud, N. J. Knowles, B. Valdazo-González, D. J. Paton, D. P. King, D. T. Haydon, Observing micro-evolutionary processes of viral populations at multiple scales. Philos. Trans. R. Soc. B 368, 20120203 (2013). doi:10.1098/rstb.2012.0203 Medline

33. N. Juleff, B. Valdazo-González, J. Wadsworth, C. F. Wright, B. Charleston, D. J. Paton, D. P. King, N. J. Knowles, Accumulation of nucleotide substitutions occurring during experimental transmission of foot-and-mouth disease virus. J. Gen. Virol. 94, 108–119 (2013). doi:10.1099/vir.0.046029-0 Medline

34. L. Ferretti, A. Di Nardo, B. Singer, L. Lasecka-Dykes, G. Logan, C. F. Wright, E. Pérez-Martín, D. P. King, T. J. Tuthill, P. Ribeca, Within-Host Recombination in the Foot-and-Mouth Disease Virus Genome. Viruses 10, 221 (2018). doi:10.3390/v10050221 Medline

35. A. D. S. Bastos, D. T. Haydon, O. Sangaré, C. I. Boshoff, J. L. Edrich, G. R. Thomson, The implications of virus diversity within the SAT 2 serotype for control of foot-and-mouth disease in sub-Saharan Africa. J. Gen. Virol. 84, 1595–1606 (2003). doi:10.1099/vir.0.18859-0 Medline

36. B. R. Beechler, C. A. Manore, B. Reininghaus, D. O'Neal, E. E. Gorsich, V. O. Ezenwa, A. E. Jolles, Enemies and turncoats: Bovine tuberculosis exposes pathogenic potential of

Rift Valley fever virus in a common host, African buffalo (Syncerus caffer). Proc. R. Soc. London Ser. B 282, 20142942 (2015). Medline

37. V. O. Ezenwa, A. E. Jolles, Opposite effects of anthelmintic treatment on microbial infection at individual versus population scales. Science 347, 175–177 (2015). doi:10.1126/science.1261714 Medline

38. P. C. Cross, J. O. Lloyd-Smith, W. M. Getz, Disentangling association patterns in fission—Fusion societies using African buffalo as an example. Anim. Behav. 69, 499–506 (2005). doi:10.1016/j.anbehav.2004.08.006

39. R. S. Spaan, C. W. Epps, V. O. Ezenwa, A. E. Jolles, Why did the buffalo cross the park? Resource shortages, but not infections, drive dispersal in female African buffalo (Syncerus caffer). Ecol. Evol. 9, 5651–5663 (2019). doi:10.1002/ece3.5145 Medline

40. E. Dyason, Summary of foot-and-mouth disease outbreaks reported in and around the Kruger National Park, South Africa, between 1970 and 2009. J. S. Afr. Vet. Assoc. 81, 201–206 (2010). doi:10.4102/jsava.v81i4.148 Medline

41. W. Vosloo, P. N. Thompson, B. Botha, R. G. Bengis, G. R. Thomson, Longitudinal study to investigate the role of impala (Aepyceros melampus) in foot-and-mouth disease maintenance in the Kruger National Park, South Africa. Transbound. Emerg. Dis. 56, 18–30 (2009). doi:10.1111/j.1865-1682.2008.01059.x Medline

42. B. P. Brito, F. Jori, R. Dwarka, F. F. Maree, L. Heath, A. M. Perez, Transmission of Foot-and-Mouth Disease SAT2 Viruses at the Wildlife-Livestock Interface of Two Major Transfrontier Conservation Areas in Southern Africa. Front. Microbiol. 7, 528 (2016). doi:10.3389/fmicb.2016.00528 Medline

43. N. Nelson, D. J. Paton, S. Gubbins, C. Colenutt, E. Brown, S. Hodgson, J. L. Gonzales, Predicting the Ability of Preclinical Diagnosis To Improve Control of Farm-to-Farm Foot-and-Mouth Disease Transmission in Cattle. J. Clin. Microbiol. 55, 1671–1681 (2017). doi:10.1128/JCM.00179-17 Medline

44. F. M. Guerra, S. Bolotin, G. Lim, J. Heffernan, S. L. Deeks, Y. Li, N. S. Crowcroft, The basic reproduction number (R0) of measles: A systematic review. Lancet Infect. Dis. 17, e420–e428 (2017). doi:10.1016/S1473-3099(17)30307-9 Medline

45. M. Kretzschmar, P. F. M. Teunis, R. G. Pebody, Incidence and reproduction numbers of pertussis: Estimates from serological and social contact data in five European countries. PLOS Med. 7, e1000291 (2010). doi:10.1371/journal.pmed.1000291 Medline

46. S. Sanche, Y. T. Lin, C. Xu, E. Romero-Severson, N. Hengartner, R. Ke, High Contagiousness and Rapid Spread of Severe Acute Respiratory Syndrome Coronavirus 2. Emerg. Infect. Dis. 26, 1470–1477 (2020). doi:10.3201/eid2607.200282 Medline

47. C. J. E. Metcalf, O. N. Bjørnstad, B. T. Grenfell, V. Andreasen, Seasonality and comparative dynamics of six childhood infections in pre-vaccination Copenhagen. Proc. R. Soc. B. 276, 4111–4118 (2009). doi:10.1098/rspb.2009.1058 Medline

48. N. Bharti, A. J. Tatem, M. J. Ferrari, R. F. Grais, A. Djibo, B. T. Grenfell, Explaining seasonal fluctuations of measles in Niger using nighttime lights imagery. Science 334, 1424–1427 (2011). doi:10.1126/science.1210554 Medline

49. M. S. Y. Lau, B. D. Dalziel, S. Funk, A. McClelland, A. Tiffany, S. Riley, C. J. E. Metcalf, B. T. Grenfell, Spatial and temporal dynamics of superspreading events in the 2014-2015 West Africa Ebola epidemic. Proc. Natl. Acad. Sci. U.S.A. 114, 2337–2342 (2017). doi:10.1073/pnas.1614595114 Medline

50. K. E. L. Worsley-Tonks, L. E. Escobar, R. Biek, M. Castaneda-Guzman, M. E. Craft, D. G. Streicker, L. A. White, N. M. Fountain-Jones, Using host traits to predict reservoir host species of rabies virus. PLOS Negl. Trop. Dis. 14, e0008940 (2020). doi:10.1371/journal.pntd.0008940 Medline

51. A. M. Kilpatrick, Globalization, land use, and the invasion of West Nile virus. Science 334, 323–327 (2011). doi:10.1126/science.1201010 Medline

52. S. Gubbins, FMDVInBuffalo, Zenodo (2021); doi:10.5281/zenodo.5121203.

53. J. Medlock, FMDV, Zenodo (2021); doi:10.5281/zenodo.5146506.

54. L. Combrink, C. K. Glidden, B. R. Beechler, B. Charleston, A. V. Koehler, D. Sisson, R. B. Gasser, A. Jabbar, A. E. Jolles, Age of first infection across a range of parasite taxa in a wild mammalian population. Biol. Lett. 16, 20190811 (2020). doi:10.1098/rsbl.2019.0811 Medline

55. C. K. Glidden, B. Beechler, P. E. Buss, B. Charleston, L.-M. de Klerk-Lorist, F. F. Maree, T. Muller, E. Pérez-Martin, K. A. Scott, O. L. van Schalkwyk, A. Jolles, Detection of Pathogen Exposure in African Buffalo Using Non-Specific Markers of Inflammation. Front. Immunol. 8, 1944 (2018). doi:10.3389/fimmu.2017.01944 Medline

56. R. S. Hedger, Foot-and-mouth disease and the African buffalo (Syncerus caffer). J. Comp. Pathol. 82, 19–28 (1972). doi:10.1016/0021-9975(72)90022-9 Medline

57. D. O. Ehizibolo, I. H. Fish, B. Brito, M. R. Bertram, A. Ardo, H. G. Ularamu, D. D. Lazarus, Y. S. Wungak, C. I. Nwosuh, G. R. Smoliga, E. J. Hartwig, S. J. Pauszek, S. Dickmu, S. Abdoulkadiri, J. Arzt, Characterization of transboundary foot-and-mouth disease viruses in Nigeria and Cameroon during 2016. Transbound. Emerg. Dis. 67, 1257–1270 (2020). doi:10.1111/tbed.13461 Medline

58. R. P. Kitching, A. I. Donaldson, Collection and transportation of specimens for vesicular virus investigation. Rev. Sci. Tech. Off. Int. Epiz 6, 263–272 (1987).

59. C. Casteleyn, S. Breugelmans, P. Simoens, W. Van den Broeck, The tonsils revisited: Review of the anatomical localization and histological characteristics of the tonsils of domestic and laboratory animals. Clin. Dev. Immunol. 2011, 472460 (2011). doi:10.1155/2011/472460 Medline

60. J. D. Callahan, F. Brown, F. A. Osorio, J. H. Sur, E. Kramer, G. W. Long, J. Lubroth, S. J. Ellis, K. S. Shoulars, K. L. Gaffney, D. L. Rock, W. M. Nelson, Use of a portable real-time reverse transcriptase-polymerase chain reaction assay for rapid detection of foot-and-mouth disease virus. J. Am. Vet. Med. Assoc. 220, 1636–1642 (2002). doi:10.2460/javma.2002.220.1636 Medline

61. C. Hamblin, I. T. Barnett, R. S. Hedger, A new enzyme-linked immunosorbent assay (ELISA) for the detection of antibodies against foot-and-mouth disease virus. I. Development and method of ELISA. J. Immunol. Methods 93, 115–121 (1986).

doi:10.1016/0022-1759(86)90441-2 Medline

62. M. Eloit, B. Schmitt, Manual of Diagnostic Tests and Vaccines for Terrestrial Animals (World Organisation for Animal Health, 2017).

63. H. Haario, E. Saksman, J. Tamminen, An adaptive Metropolis algorithm. Bernoulli 7, 223–242 (2001). doi:10.2307/3318737

64. C. Andrieu, J. Thoms, A tutorial on adaptive MCMC. Stat. Comput. 18, 343–373 (2008). doi:10.1007/s11222-008-9110-y

65. M. Plummer, N. Best, K. Cowles, K. Vines, CODA: Convergence diagnosis and output analysis for MCMC. R News 6, 7–11 (2006).

66. R Core Team, R: A language and environment for statistical computing (R Foundation for Statistical Computing, 2013); www.R-project.org/.

67. D. J. Spiegelhalter, N. G. Best, B. P. Carlin, A. van der Linde, Bayesian measures of model complexity and fit. J. R. Stat. Soc. Ser. B 64, 583–639 (2002). doi:10.1111/1467-9868.00353

68. M. J. Keeling, P. Rohani, Modeling Infectious Diseases in Humans and Animals (Princeton Univ. Press, 2008) doi:10.1515/9781400841035

69. S. Yadav, C. Stenfeldt, M. A. Branan, K. I. Moreno-Torres, L. K. Holmstrom, A. H. Delgado, J. Arzt, Parameterization of the Durations of Phases of Foot-And-Mouth Disease in Cattle. Front. Vet. Sci. 6, 263 (2019). doi:10.3389/fvets.2019.00263 Medline

70. G. Celeux, F. Forbes, C. P. Robert, D. M. Titterington, Deviance information criteria for missing data models. 1, 651–673 (2006). doi:10.1214/06-BA122

71. A. Gelman, J. Hwang, A. Vehtari, Understanding predictive information criteria for Bayesian models. Stat. Comput. 24, 997–1016 (2014). doi:10.1007/s11222-013-9416-2

72. A. Vehtari, A. Gelman, J. Gabry, Practical Bayesian model evaluation using leave-one-out cross-validation and WAIC. Stat. Comput. 27, 1413–1432 (2017). doi:10.1007/s11222-016-9696-4

73. Python Core Team, Python: A dynamic, open-source programming language (2020); https://www.python.org/.

74. E. Jones, T. Oliphant, P. Peterson, SciPy: Open source scientific tools for Python (2001); https://www.scipy.org/.

75. R. Y. Rubinstein, Simulation and the Monte Carlo Method (Wiley, 1981).

76. D. T. Gillespie, Exact stochastic simulation of coupled chemical reactions. J. Phys. Chem. 81, 2340–2361 (1977). doi:10.1021/j100540a008

77. S. M. Blower, H. Dowlatabadi, Sensitivity and uncertainty analysis of complex models of disease transmission: An HIV model, as an example. Int. Stat. Rev. 62, 229–243 (1994). doi:10.2307/1403510

78. S. Marino, I. B. Hogue, C. J. Ray, D. E. Kirschner, A methodology for performing global uncertainty and sensitivity analysis in systems biology. J. Theor. Biol. 254, 178–196 (2008). doi:10.1016/j.jtbi.2008.04.011 Medline

79. P. C. Cross, D. M. Heisey, J. A. Bowers, C. T. Hay, J. Wolhuter, P. Buss, M. Hofmeyr, A. L. Michel, R. G. Bengis, T. L. F. Bird, J. T. Du Toit, W. M. Getz, Disease, predation and demography: Assessing the impacts of bovine tuberculosis on African buffalo by monitoring at individual and population levels. J. Appl. Ecol. 46, 467–475 (2009). doi:10.1111/j.1365-2664.2008.01589.x

80. T. E. Harris, The Theory of Branching Processes (Springer, 1963).

81. M. Kot, Elements of Mathematical Ecology (Cambridge Univ. Press, 2001).

82. T. S. Parker, L. O. Chua, Practical Numerical Algorithms for Chaotic Systems (Springer, ed. 3, 1992).

83. F. A. Milner, G. Rabbiolo, Rapidly converging numerical algorithms for models of population dynamics. J. Math. Biol. 30, 733–753 (1992). doi:10.1007/BF00173266 Medline